Appl Phys A (2012) 106:339–361
DOI 10.1007/s00339-011-6699-z

Applied Physics A
Materials Science & Processing

INVITED PAPER

Laser spectroscopies for elemental and molecular analysis in art and archaeology

Austin Nevin · Giuseppe Spoto · Demetrios Anglos

Received: 31 March 2011 / Accepted: 7 November 2011 / Published online: 6 December 2011
© Springer-Verlag 2011

Abstract Spectroscopic methods using laser sources have significantly improved our capacity to unravel the chemical composition of works of art and archaeological remains. Lasers enhance the performance of spectroscopic techniques which require intense light sources and specific analytical protocols assuring a microanalytical approach for analysis has been established. This review focuses on laser spectroscopic methods used in the field of cultural heritage diagnostics. Emphasis in this work is given to the analytical capabilities of laser-based techniques for elemental and/or molecular analysis and in-situ use, spatial resolution and microanalysis. Analytical methods are classified according to the elemental (LIBS, LA–ICP–MS) and molecular (LIF/LIDAR, time-resolved absorption spectroscopy, laser desorption ionization mass spectrometry) information they yield. For non-destructive laser-induced fluorescence (LIF/LIDAR) and time-resolved fluorescence spectroscopy, imaging applications are described. The advantages provided by combined complementary techniques including but not limited to LIBS–LIF–Raman and LIBS–XRF are presented, as are recent improvements in terms of chemical imaging. Advances and applications of THz spectroscopy, non-linear spectroscopy and imaging are outlined. Finally, laser spectroscopies are described for investigations of different materials and works of art which include Bronze Age ceramics, Minoan archaeological remains, Ancient Roman buildings, Renaissance wall paintings and sculptures, and manuscripts containing iron gall inks and colorants.

A. Nevin
Dipartimento di Fisica, Politecnico di Milano, Piazza Leonardo da Vinci 32, 20133 Milan, Italy
e-mail: austinnevin@gmail.com

G. Spoto
Dipartimento di Scienze Chimiche, Università di Catania, Viale A. Doria 6, 95125 Catania, Italy
e-mail: gspoto@unict.it

D. Anglos (✉)
Institute of Electronic Structure and Laser, Foundation for Research and Technology–Hellas, P.O. Box 1385, 71110 Heraklion, Crete, Greece
e-mail: anglos@iesl.forth.gr

D. Anglos
Department of Chemistry, University of Crete, P.O. Box 2203, 71003 Heraklion, Crete, Greece

1 Introduction

Spectroscopic methods used in art and archaeology may provide a wealth of information about samples with complex chemical compositions. In the past, artifacts or archaeological objects were manufactured by manipulating natural products which were often a mixture of both organic and inorganic compounds. In parallel, synthetic inorganic and organic materials have been used for painting and their inclusion in modern works of art make conservation and analysis a particular challenge. Additionally, the chemical complexity of mixtures is further increased by the altering processes that intervene in the life cycle of historical objects. It is for these reasons that powerful analytical tools are required to study art and archaeological materials.

Laser spectroscopies play an important role in the analysis of art and archaeological objects. In fact, they can be used to identify both the inorganic and organic components with high sensitivity and reproducibility. Moreover, laser spectroscopies provide new opportunities for microanalytical and, at times, completely non-destructive analyses, thus opening up new diagnostic approaches for the study of precious samples and works of art. In particular, through using laser

spectroscopies it is possible to extract information from different points and areas on an object; important issues can be addressed when valuable heterogeneous pieces of art or archaeological remains are chemically analyzed using laser spectroscopies. Most of the spatially resolved laser spectroscopies applied in the study of works of art and archaeological materials involve probing samples with laser radiation and simultaneously measuring the energy distribution of a specific class of emitted or scattered particles. Moreover, depth resolution is also used to characterize the vertical performance of surface-sensitive laser spectroscopies.

Since the advent of various types of laser spectroscopies in the 1960s and 1970s [19], studies focusing on the analysis of materials in works of art and archaeological remains have been increasingly published and this work attempts to present and discuss an overview of the results achieved. In particular, laser spectroscopic methods can be classified according to their ability to unravel the elemental (LIBS, LA–ICP–MS) and molecular (LIF/LIDAR, Raman spectroscopy, time-resolved absorption spectroscopy, laser desorption ionization mass spectrometry) compositions of the analyzed objects. Emphasis is also given to combined techniques which serve to expand the potential of the analytical approach adopted.

Table 1 shows the typical lateral resolution and depth of penetration for most of the spatially resolved laser spectroscopies discussed in this review with other information related to the sample size requirements of the method and the scanned area. The latter information is important in order to evaluate the volume of the 3D objects that can be analyzed with each technique. Laser spectroscopies here discussed do not include Raman spectroscopy; readers interested in the application of Raman spectroscopy in art and archaeology are addressed to an excellent review provided on this topic [171].

2 Elemental analysis

Offering straightforward qualitative and quantitative information on the composition of materials, elemental analysis methods have long been used in archaeological research and conservation science as a primary tool in the characterization and study of many objects and works of art [27, 120, 139, 160]. The identity and composition of a broad variety of materials including pigments and minerals, metal alloys and jewelry, stone and glass, pottery and soil can be determined by the use of well-known elemental analysis techniques including X-ray fluorescence (XRF) spectrometry [91, 114], particle-induced X-ray emission (PIXE) [46], electron microscopy coupled to X-ray microanalysis [160], atomic absorption/emission spectrometry or inductively coupled plasma mass spectrometry (ICP–MS) [76]. With the exception of XRF and, in part, PIXE, the rest of the techniques listed above require sampling and sample preparation, which can often involve elaborate chemical procedures.

This is actually where lasers come in [77]. Irradiation of a solid surface with a pulsed laser beam, above a certain energy density threshold, leads to material desorption or ablative breakdown and plasma excitation. This constitutes a unique microsampling tool that can be combined either with atomic emission spectrometry, giving rise to LIBS (laser-induced breakdown spectroscopy), or with mass spectrometry (MS) in two different modes leading to laser desorption ionization (LDI)–MS or laser ablation inductively coupled plasma (LA–ICP)–MS. In LDI–MS pulsed laser irradiation leads to gentle sampling that enables desorption of intact analyte molecules from a surface/matrix (details are discussed in Sect. 3.2). In LA–ICP–MS the laser acts primarily as a microsampling and material breakdown tool feeding the ICP, while in LIBS the pulse, in addition to sampling and breakdown, leads to plasma formation and excitation. In the following sections, information obtained through the use of LA–ICP–MS and LIBS is described.

2.1 LIBS

Laser-induced breakdown spectroscopy, also known as laser-induced plasma spectroscopy (LIPS), enables the determination of material elemental composition on the basis of the characteristic emission from atomic species in a microplasma that is produced by focusing a pulsed laser on the surface of a solid sample/object [37]. LIBS has been used in a wide variety of analytical applications for the qualitative, semi-quantitative and quantitative analysis of materials and offers certain features which are quite important in the context of cultural heritage materials analysis [5, 69]. It is a straightforward, versatile and simple analytical technique, which can be employed even by non-specialized users. LIBS is fast and provides results in real time, which is important when decisions for further action need to be made, for instance how to proceed with an excavation or how to deal with object conservation. More importantly, LIBS is applicable in situ—that is, on the object itself—and, because of the tight beam focusing, it ensures good spatial resolution with spot sizes invisible to the naked eye (microdestructive). Additionally, all these features are now combined in compact portable units that offer versatility and enable the use of LIBS for the analysis of a broad variety of objects/samples at diverse locations [2, 59].

2.1.1 Physical principles and instrumentation

The main steps in LIBS analysis include laser irradiation of the sample surface leading to plasma formation followed

Table 1 Summary of some relevant characteristics of the discussed laser spectroscopies (laser-induced fluorescence (LIF), time-resolved absorption spectroscopy (TRS), fluorescence lifetime imaging (FLIM), THz spectroscopy (terahertz spectroscopy), laser ablation inductively coupled plasma mass spectrometry (LA–ICP), laser-induced breakdown spectroscopy (LIBS), laser desorption ionization–ultraviolet mass spectrometry (LDI–UV), matrix-assisted laser desorption ionization–infrared (MALDI–IR), atmospheric pressure–MALDI (AP–MALDI))

	Typical lateral resolution	Typical depth of penetration	Typical XYZ movable range[b]	Operating conditions	Removed material	Applications
LIF spectroscopy	1–5 mm	Surface	XY = variable	Atmospheric pressure	None	Analysis of minerals, pigments, varnishes binding media, organisms
TRS	1 mm	0.5–1 cm	XY = variable	Atmospheric pressure	None	Analysis of components of wood, assessment of scattering and absorption coefficients
FLIM	30 cm	Surface	XYZ = variable	Atmospheric pressure	None	Imaging of fluorescence lifetime of surfaces
THz spectroscopy	≤50 mm [63, 113]	Transmission or reflectance analysis	Fixed position	RH ≤ 10%, atmospheric pressure	None	Analysis of pigments, binding media, water content
LA–ICP	5–300 µm [145]	~100 nm per laser pulse [145]	XY = 5 cm Z = 2 cm	760 torr, argon gas	50–500 µg	Trace element and isotope analysis of metals, pottery, minerals
Micro LIBS	3–15 µm [119]	100–500 nm [135]	XYZ = 20 cm	760 torr	0.01–0.2 µg [69]	Elemental analysis of metals, pottery, glass, stone, soil, pigments
LDI–UV	200–500 µm	50–200 nm[a] [47]	XY = 20 cm Z = 0	10^{-7}–10^{-8} torr	Few tens of micrograms of material is sampled from the object to be analyzed [98]	Analysis of organic and inorganic pigments and dyes
MALDI–IR	100–300 µm [47, 48]	1.5–2.0 µm [47]	XY = 20 cm Z = 0	10^{-7}–10^{-8} torr	Femtomoles per laser pulse [92]	Analysis of organic components and residues
AP–MALDI	~400 µm [70]	50–200 nm [47]	XZ = 50 cm Y = 30 cm[c]	760 torr	0.3–3 nmoles mm^2 [70]	Analysis of organic components: pigments, dyes, binders, resins

[a]Most of the LDI–MS experiments have been carried out by using standard MALDI equipment. For this reason lateral and depth resolutions similar to MALDI are obtained. Improved performances in terms of lateral resolution have been obtained by using specifically designed laser microprobe equipment (see Ref. [47])

[b]The values shown refer to standard commercial equipment

[c]The reported values refer to equipment specifically designed for the analysis of art objects (see Ref. [70])

by optical detection/recording of the wavelength-resolved plasma emission, preferably in a time-resolved manner, and finally analysis/interpretation of the spectral data.

Prior to irradiation, the spot to be analyzed on the sample/object is selected. This is fundamental for carrying out meaningful analysis, given the vast surface and bulk heterogeneity of excavated objects or works of art. A simple camera is often of great help for achieving proper positioning of the sample with respect to the focused laser beam. The LIBS measurement starts by irradiating the object surface with one or more laser pulses through a focusing lens that concentrates light down to a spot of diameter in the range of 20–200 µm. Typically, nanosecond-pulsed lasers are used, with the one of choice being a Q-switched Nd:YAG laser emitting at its fundamental (1064 nm) or its harmonics (532, 355, 266 nm). Other nano- as well as pico- and femtosecond pulsed lasers have been used, but mostly in research studies. The laser wavelength is a critical parameter, which, in

combination with material absorptivity and scattering, determines the coupling of the irradiation to the material surface. Strong absorption confines sampling to a very thin layer, in the range of 0.1–1 μm, minimizing material removal and enhancing depth resolution. The quality of the laser beam is important both for minimizing the affected surface area and for obtaining good lateral spatial resolution. Typical values of the laser pulse energy lie in the range of 1–30 mJ, which translate to energy density values on the sample surface in the range of 1–50 J cm^{-2} (0.1–5 × 10^9 W cm^{-2}). Nanosecond laser irradiation results in a rapid deposition of energy on the sample surface (within a minute volume of material, less than 0.1 mm^3) leading, through a series of processes, to material breakdown and generation of a microplasma plume just above the irradiated spot. With time, typically a few hundred nanoseconds following the end of the laser pulse, the plasma expands and cools down giving rise to strong emission with sharply peaked spectral features, arising from the excited atomic species, neutrals and ions, in the plume. Fiber optics, often with the aid of lenses, are typically employed to collect the plume emission into a spectrograph, where light is analyzed and recorded on the detection system, a gated CCD. Gating the detector permits time-resolved recording of the plasma emission; this is important for rejecting the very strong continuum background present at the early times of laser plasma formation.

Qualitative analysis is quite straightforward and is done by assigning the distinct sharp atomic emission peaks in the spectrum to the corresponding elements. This is facilitated by use of spectral libraries, nowadays available on a PC or accessible over the Internet. It is emphasized that in most cases a single laser pulse is sufficient to produce a clean spectrum which can lead to quick determination of the qualitative (and often semi-quantitative) composition of the sample. Here, it is important to consider the laser beam confinement in a relatively thin layer of material and how this might affect the analytical information. If superficial impurities are present or the sample has a multi-layer stratigraphy (both situations are quite common in cultural heritage objects), single-pulse spectra reflect precisely the composition of the sample layers probed. Surface-corroded metals, stone and pottery bearing burial deposits and multi-layer paints represent just some relevant examples. Taking advantage of the confined ablation depth per pulse it is straightforward to realize that multiple pulses, namely successive LIBS measurements on the same spot, lead to depth profiling of the sample, particularly useful when complex stratigraphies are encountered.

Quantitative analysis, obviously quite important in many compositional analysis problems, is based on relating the (integrated) intensity of a spectral line to the number density of each emitting species in the plume and this, in turn, with the concentrations of specific elements in the solid. Commonly, quantitative analysis is performed by analyzing samples against calibration standards of known analyte composition, following the calibration curve method. Given the different types of surfaces encountered, their varying compositions and material heterogeneity, it is not always feasible to obtain proper standards for comparison. In certain cases, reliable calibration-free LIBS methods have been proposed and used [28].

Some interesting variations of LIBS have been proposed that are promising with respect to improving or extending the applications of LIBS. These include double-pulse LIBS, shown to lead to enhanced analytical sensitivity [153], or open-path remote LIBS that could be appropriate for large surface scanning of monuments and buildings from stand-off distances [81, 134, 168].

2.1.2 *Applications of LIBS*

2.1.2.1 Metals and metal alloys The strong coupling of ns pulses to metallic substrates, regardless of laser wavelength (UV to NIR), makes LIBS quite an efficient method for the analysis of metals and metal alloys and thus suitable for the characterization of archaeological and historical metallic artifacts such as sculpture, tools, weapons, home utensils, jewelry and coins. The main metallic materials used in antiquity include copper and bronze—copper–tin alloys (starting in the Bronze Age)—and later iron. Other metals used include lead and zinc while precious metals such as silver or gold alloys are more often associated with jewelry and for decorating different objects.

Simple, qualitative LIBS analysis can be a helpful tool for quickly classifying or discriminating among like objects, for instance various types of bronze materials or different types of coins. More importantly, quantitative analysis of metal alloys can reveal valuable information about metallurgical technology, period of manufacture and possibly provenance of the raw materials on the basis of the major, minor and trace elements detected. For example, by means of quantitative LIBS analysis it was possible to obtain a chronological classification of a number of bronze objects from the Iberian peninsula, dating from the Bronze to the Iron Age, on the basis of the elemental content of the alloys and particularly the concentration of arsenic (As), the presence of which is a key indicator of the Early Bronze Age [58]. Cluster analysis enabled reliable sorting of the objects across the different periods. In a similar study [36], archaeological bronze artifacts from a burial site in Southern Tuscany, Italy, dated in the period of 2500–2000 B.C.E. were examined using micro-LIBS analysis and by use of the calibration-free LIBS method concentrations of the elements in the alloy were obtained. These results, with the help of principal component analysis (PCA), led to a typological grouping of the objects

and in certain cases indicated a classification different from that suggested by the traditional typology, offering archaeologists a more thorough perspective into the origin and use of the objects. The quantitative analysis of metals can be clearly extended to studies of jewelry as well [35].

LIBS also enables analysis of superficial contamination and corrosion layers on metal artifacts providing information about object burial history or informing about certain types of corrosion that might require specific conservation treatment. A thin corrosion layer is usually etched away following irradiation with a small number of pulses allowing the laser beam to probe the bulk metal. However, if thick corrosion layers are present, analysis results have to be interpreted with caution unless it is certain that the laser beam has actually reached the bulk metal. In this context, LIBS has also been used to monitor metal objects during laser cleaning. For example, laser cleaning of a heavily corroded bronze gun, found in the Adriatic seabed (16th–17th century C.E.), has been evaluated using qualitative LIBS analysis revealing a significant reduction of calcium emission upon removal of the encrustation layer [1].

In a more demanding type of application, relating to marine archaeology, double-pulse LIBS has been conducted successfully for the analysis of metal objects submerged in water including iron, copper-based alloys and precious alloys that resemble in composition archaeological ones [43, 108].

2.1.2.2 Marble and stone Analysis of marble and stone can be useful in provenance studies or in determining the type of surface encrustations and relating those to specific burial environments in the case of excavated objects or to pollution processes in sculpture and monuments exposed to urban environment. The possibility to carry out LIBS analysis without the need of collecting samples is quite important particularly if portable equipment enables analysis on location.

In a detailed study [107], LIBS has been employed in the analysis of different white marble types (from Naxos (Greece), Proconnesos (Turkey) and Carrara (Italy)) both in the bulk stone and on the surface encrustation. Quantitative analysis data was obtained for the main constituents (Ca, C, Al and Si) as well as for impurity elements (Fe, Mg, Mn, Ti, Ba and Cu) present at the ppm level with the help of reference samples based on $CaCO_3$ matrices doped with certified soils.

An important question in the conservation of stone sculpture relates to the determination of the thickness of the pollution crusts and the distribution of certain pollutants as a function of depth from the surface. In this context, a depth profiling study can be quite illuminating: it has been shown that in LIBS analysis of marble encrustation, emissions from several elements, which originate from the environmental deposits including Fe, Al, Si and Ti, are detected in contrast to the unweathered marble, which contained these elements at much lower levels [116].

Various types of geological materials have been used in early times to make simple tools and sculpture. Their elemental composition, and particularly that of minor and trace elements, has been related to provenance of the object. In this respect, such analysis can be of importance in uncovering, for example, the sources of raw materials used to make certain objects by comparison of compositional patterns between the object in question and the original raw materials. Quick screening can be performed on the basis of qualitative analysis, if differences in elemental content are significant [84]. For more detailed studies a systematic quantitative analysis of major and minor components is obviously needed [39].

2.1.2.3 Pottery and ceramic objects Ceramic objects are the most common among archaeological and historical findings. Analysis of the fabric (main body of the ceramic) provides evidence about the clay composition revealing technological and potentially provenance information. Surface analysis may yield artistic and technological information concerning the slip (original paint layer) or the glaze in the case of glazed pottery. LIBS has been used in several studies of pottery such as, for example, the characterization of a collection of ancient Roman pottery sherds, *Hispanic Terra Sigillata*, that originated from different production sites and dated back to the 1st–5th century C.E. On the basis of the elemental content of sherds and with the aid of linear correlation analysis of LIBS spectra, it was possible to classify the sherds according to their production location. Furthermore, depth profiling studies were carried out in order to distinguish between the slip and the fabric of the ceramic sherds and elements such as calcium and iron were used as markers for the transition from the one layer to the other [111]. Likewise [9], linear and rank correlation methods have been applied successfully for the characterization of various ceramic samples (archaeological and modern). In a similar study [54], selected pottery sherds coming from three different excavations in eastern Turkey and dated from the Early to Middle Iron Age were examined as regards to their composition by using LIBS. Comparison of results from LIBS from analysis of the colored slip (paint layer) and on the fabric (bulk ceramic) revealed a strong correlation of the red color with the iron (Fe) content of the slip layer. Furthermore, test studies, using PCA on LIBS spectra, showed that the analytical information contained in the raw spectral data (no quantitative analysis done) can be used for differentiating among sherds coming from different sites known to have used different clay sources and pottery making technology.

2.1.2.4 Glass and faience Vitreous materials (faience, glass and glaze) are made of quartz (or quartz sand), lime,

alkalies (soda or potash) and metal oxides. Chemical analysis of ancient glass is a way to reveal the composition, selection of raw materials, as well as the coloring agents. Furthermore, the analysis of weathered glass helps to study the decay processes and understand mechanisms.

In this context, a thorough study undertaken has examined the potential of LIBS in the analysis of historical glasses [127]. Measurements on a series of certified standard glass samples using a commercial LIBS instrument based on an echelle spectrometer (and using ns laser pulses at 266 nm) gave, for most elements, satisfactory I values with precision in the range of 3–20%. More research is clearly required to improve the precision by optimizing measurement conditions as well as corrections related to plasma temperature and electron density variations given the fact that glasses exhibit rather weak absorption even in the UV. In a different study [23], artificially weathered glass samples (similar to the composition of original glasses from Medieval and Renaissance periods) as well as commercially available 'antique' glasses with a modern chemical composition and coloring components (the chromophores) were examined by LIBS. The analysis of their main components was carried out successfully while the presence of trace elements (Co, Cu, Mn, Fe and Cr) was attributed to different types of chromophores based on ions of the above transition metals. Weathered glass consists of the unaltered bulk glass material, a hydration layer created through the exchange between alkali and hydrogen ions (as a consequence of the water diffusion from environment), and may also present a layer of externally formed corrosion salts. Depth profiling by LIBS gave a qualitative indication regarding the profiles of the different corrosion layers of the artificially weathered glass samples.

Turning to much older artifacts made of faience, a few Bronze Age objects (found in Crete, Greece) such as beads, vessels and decorative objects were analyzed using LIBS in order to identify glaze colorants and surface decorations. The color of the glaze was correlated with certain metals such as for example manganese for brown, copper and manganese for green while noble metal coatings made of gold or silver were also identified. In one of the faience beads examined for determining the pigment decoration used on its surface, the emission recorded indicated actually the presence of silver on the surface proving that the grey material covering the bead was not a pigment but the remainder of a corroded silver coating [118].

2.1.2.5 Pigments Among the most attractive applications of LIBS (Fig. 1) in the context of applications in art and archaeology has been the study of pigments in various forms of painted artwork such as easel and wall paintings, wood and metal polychromes, illuminated manuscripts and pottery [5, 21, 22]. Most pigments used in paintings (from antiquity to relatively modern times) are inorganic compounds

Fig. 1 Analysis of a painting with a compact portable LIBS spectrometer. (A probe head unit, containing a small nanosecond Nd:YAG laser, is positioned, with the aid of a micropositioning stage, over the painting. The LIBS emission signal is collected through the optical head and by optical fibers transmitted to a compact grating spectrograph equipped with a gated CCD detector controlled through a laptop computer [175])

that have been either naturally available as colored minerals or synthetic ones. In several cases pigment identification is quite straightforward on the basis of the metallic elements detected through LIBS and the paint color. Obviously, unambiguous identification is not always possible. For example, detecting copper (Cu) in a green paint might be related to the use of more than one copper-based green pigment (e.g. malachite, verdigris, copper resinate) and in that case additional data from a molecular analysis technique, for example Raman spectra, could clarify the result.

2.1.2.6 Biomaterials Analysis of biomaterials is an area of potential interest to archaeological research focused on human remains, aiming to identify certain diseases, nutritional habits or deficiencies or the presence of potentially toxic elements or animal remains and fossils. The characterization of calcified tissues employing LIBS is an example of such a quantitative analysis of traces of aluminium, strontium and lead in human bones or teeth [151]. It was demonstrated in that study that the above trace elements can be quantitatively detected and, in fact, surface mapped in calcified tissue samples. These results indicate strongly the potential advantages of LIBS in the analysis of bio-archaeological samples.

In a different type of study, samples of parchment (collagen) from different sources were analyzed by LIBS and, on the basis of the concentrations of a number of elements (Ca, Na, K, Mg, Fe, Cu and Mn), it became possible to achieve a clear discrimination between modern and historical samples. Furthermore, correlations were found between the animal type and the ratio of Mg:Cu emission lines intensity [45].

Organic analysis in biomaterials is more challenging; although light elements present in organic materials such as

carbon, hydrogen and oxygen can be detected by LIBS, results may lead to non-reliable conclusions about their exact concentrations in the sample (due to their existence in air atmosphere and interaction with the atmospheric molecules). In an interesting approach [163], LIBS was used to examine fossilized buffalo horns from Indonesia, 400,000 and 1,000,000 years old, under reduced ambient pressure (3 torr). The low-pressure surrounding gas is crucial for overcoming the undesirable broadening effect and the resulting decrease in hydrogen and carbon emission efficiencies that occur at atmospheric pressure, conditions that are common in regular LIBS analysis. The carbon and hydrogen line intensities were used as indicators of the fossilization degree of the samples and thus of their age (no carbon signal was detected in the older samples). Using the same technique [109], analysis of fresh and fossilized corals and shells was performed in an effort to establish a method for discriminating between original and artificial materials used for fabricating beads used in a religious context. Emissions (from C, H, Na, Mg and Ca) were proposed as indicators for distinguishing between original and imitation materials or between fresh and fossilized coral beads.

2.1.2.7 Laser cleaning In the past two decades laser ablation, because of its precise material removal features, has been introduced as a tool in art conservation. Many different objects, including marble, stone sculpture, various metal artifacts, stained glass, paintings, icons and works of art on paper, have been investigated with laser ablation cleaning [33, 60, 141, 155]. The cleaning process relies on the controlled removal of contaminants or other unwanted materials from the object surface by means of laser ablation. A critical issue regarding the success of the cleaning process relates to knowing where (and when) to stop the process. That is, to be able to assess reliably to what extent the undesirable material has been removed. Such control of laser cleaning can be achieved, in certain cases, by monitoring the optical emission resulting from material ablation. In essence, a LIBS measurement is carried out simultaneously with the laser cleaning. As already discussed, successive laser pulses on the same spot can provide compositional information about the surface and into the bulk material. If distinct differences exist between the LIBS spectra of the contamination layer to be removed and the original surface, then it is, in principle, possible to control the process of cleaning by an algorithm implemented on a computer. Such control of laser cleaning has been demonstrated in several cases including the removal of overpaint from wall paintings [72] and of encrustation from marble [115, 150] or glass. For example, LIBS was used to control the cleaning process of medieval stained glass [99] monitoring the elemental composition of the crust during the cleaning process. An increase of magnesium and silicon with a synchronous decrease of calcium was observed as the ablation proceeded towards the bulk glass material. Therefore, the relative intensities of Si/Al emission were selected as critical parameters capable of signaling the end point of the cleaning process.

2.2 Laser ablation inductively coupled plasma mass spectrometry

Material ablation, which is observed upon irradiation of condensed phases with laser pulses at high laser irradiances ($>10^6$ W cm^{-2}) [67], has been proposed as a solid sampling technique for inductively coupled plasma mass spectrometry (ICP–MS) since 1985 [77]. An IR ruby laser operating with laser pulse energy of 0.3–1 J was used to irradiate a standard rock sample and the ablated material was transferred into the plasma of an ICP source in order to generate atomic ions. Today Nd:YAG (1064, 532, 266 or 213 nm), ArF excimer (193 nm; this is the most widely used wavelength) and, more recently, fs Ti:sapphire (800 or 193 nm) [49, 55] lasers provide more stable sources for material ablation from solid samples. Upon laser irradiation, material is removed under vapor or solid (particles or agglomerates) forms and is transported to the ICP source with the assistance of an Ar or He gas flow via a simple polymeric tubing. The interaction of the ejected material with the plasma of the ICP source led to its vaporization, atomization and ionization. The formed ions are extracted from the plasma and introduced into the mass analyzer that separates ions according to their mass-to-charge ratio. Common interfering species formed in the plasma are charged oxides (MO^+), halides (MH^+) and argides (MAr^+). Also, a common problem encountered in laser ablation sampling is elemental fractionation. The latter results in detection of ionic species which are not fully representative of the solid sample composition and has been shown to be dependent on laser wavelength [90]. UV lasers help to reduce fractionation, since atomic and ionic species are formed with improved efficiency in comparison to IR lasers [149].

2.2.1 Applications of LA–ICP–MS

LA–ICP–MS has been used mostly to explore the elemental and isotopic composition of a variety of artistic or archaeological samples. A detailed list of applications of LA–ICP–MS in the field may be found elsewhere [71, 145].

Metallic objects, ceramics and glasses have been investigated for fingerprinting purposes operating under either line-profiling or drilling-at-one-spot modes. Line-profile analysis is preferred when flat samples are to be analyzed and benefits from the reduced elemental fractionation and the enhanced sensitivity. It has been used to evaluate the elemental distribution across the surface of written documents [173] and also to analyze skeletal remains supposedly connected

to Mozart and to suspected relatives [161]. The drilling-at-one-spot mode, which is the most widely adopted operative protocol in LA–ICP–MS, minimizes sample alterations and maximizes spatial resolution (Table 1). Applications include the analysis of ancient coins [152], glazed ceramics [136] and pigments used in prehistoric rock art [144].

LA–ICP–MS qualitative elemental fingerprint analysis has been shown to be useful for provenance and authentication of indigenous art [78]. However, quantitative analysis represents the principal expected application for each ICP–MS-based technique. LA–ICP–MS quantitative analysis applications are limited by calibration issues caused by the difficulty to obtain reliable solid standards. Glass and metal samples are more frequently quantitatively analyzed due to the wider availability of reference materials with bulk composition similar to that of the sample to be analyzed. When the sample bulk composition differs significantly from the standard, it is a good practice to use an internal reference element to partially compensate for differences between sample and standard. Some authors have reported the use of home-made standards for the quantitative analysis of stone materials [169].

The determination of isotope ratios for selected elements is also achieved through LA–ICP–MS. Ratios of Pb, Sr or U isotopes are evaluated for establishing provenance and dating. Applications of this technique have been suggested in archaeometric studies and involve coins and metal samples, glasses and ceramics [145].

2.2.1.1 Metals and metal alloys LA–ICP–MS elemental qualitative fingerprint and quantitative analyses of metal objects have been widely used for establishing provenance. Provenancing precious metals like gold and silver has been a challenging task since trace elemental analysis has been affirmed and applications of LA–ICP–MS in provenancing gold artifacts have been reported [82]. Recently, analysis by LA–ICP–MS (with a fs Ti:sapphire laser operating at 266 nm) of major, minor and trace element in Chinese gold objects in the Smithsonian's Freer Gallery of Art and Arthur M. Sackler Gallery has shown that association of silver with trace palladium, platinum, tin, copper and zinc led to patterns useful for fingerprinting [20]. Copper-based alloys were also investigated with the aim to discriminate between different copper sources [50] while lead isotopic analyses of copper and silver ingots have been performed by using multi-collector mass spectrometers [11].

2.2.1.2 Glasses and glazes LA–ICP–MS is a powerful analytical tool for discriminating glassy archaeological materials. For example, archaeological glass beads originating from south Asia and sub-Saharan Africa were successfully discriminated on the basis of a low-uranium/high-barium ratio associated to an early period in Sri Lanka and South India, versus a high-uranium/low-barium ratio that was relevant to glass produced on the west coast of India and in sub-Saharan Africa after the 9th century C.E. [51]. With a pretty similar analytical approach, also Egyptian and Mesopotamian blue and colorless glasses were discriminated because the LA–ICP–MS supported the conclusions that different raw materials and/or manufacturing processes were used [154].

2.2.1.3 Obsidian Obsidian is a glassy material formed during solidification of magmatic flows. Obsidians have been analyzed by using LA–ICP–MS for establishing their provenance. Analyses of obsidian objects with different geographic origins have been carried out [71] by selecting the elements that better discriminate between sources. The quantitative evaluation of elements like barium and the rare earths (REs) and ratios like Zr/Y and Zr/Nb are frequently used to discriminate between different obsidian sources. However, it has been demonstrated that the LA–ICP–MS quantitative evaluation of other elements can also be used successfully for provenancing purposes [176].

3 Molecular analyses

Objects like paintings, sculpture, textiles, books, furniture and archaeological remains consist of a complex mixture of inorganic and organic molecular systems whose identification requires powerful analytical approaches.

The identification of molecular components of works of art and archaeological objects has been a challenge since the 1970s when traditional instrumental analytical methods were first used with this aim. Since then, molecular analytical techniques have been used in art conservation and archaeological science with a variety of purposes. The identification of the chemical composition or nature of the material under study; the evaluation of the state of alteration of the objects caused by the long-term exposure to the environment; and the study of the effects of restoration procedures are some of them.

Laser spectroscopies have been widely used in order to achieve the aims mentioned above. The interaction between the laser radiation and the object under study can provide compositional information on the basis of the electronic or vibrational structure of molecular systems reflected in their corresponding optical spectra. In addition, charged fragments or molecular ions can also be desorbed from the sample surface and mass analyzed. Both the phenomena are exploited to characterize or identify a variety of materials including stone, pigments and dyes, glasses, binding media and varnishes.

The following sections discuss the use of laser spectroscopic molecular techniques in the study of art and archaeological objects with particular emphasis on laser-induced

fluorescence and laser desorption ionization mass spectrometry.

3.1 Laser-induced fluorescence

Laser-induced-fluorescence (LIF) spectroscopy is a specific class of fluorescence or luminescence spectroscopy making use of a coherent monochromatic laser source, in pulsed or continuous operation, as an excitation source. Luminescence (and more often fluorescence) spectroscopy has found many applications in the analysis of works of art, cultural heritage and their constituent materials. Defined as the spontaneous emission of radiation from an electronically excited species, fluorescence has long been used for the examination of works of art. With advances and wider use of non-destructive fluorescence spectroscopy for the analysis of cultural heritage [147, 166], there has been an increase in applications of LIF spectroscopy and laser-based fluorescence imaging techniques for analysis of cultural heritage [8].

The section below focuses exclusively on LIF. Distinct advantages are provided with LIF with respect to lamp-based fluorescence spectroscopy; lasers are more easily manipulated, they are sufficiently coherent and bright to allow remote analysis and pulsed sources can be used for time-resolved analysis. In addition, scattering associated with LIF is more easily filtered, making analysis of heterogeneous surfaces much more straightforward.

It is worth noting that various terms are used in the scientific literature to indicate analyses performed with LIF spectroscopy, and many not explicitly; these include photoluminescence [105, 142], laser-induced luminescence [15] and laser-induced microphotoluminescence [137, 138] spectroscopies. A distinction is not always made in the literature to indicate when laser sources are employed for fluorescence, and whether analysis yields spectrally and/or time-resolved information, but results discussed below will indicate when time-resolved fluorescence spectroscopy has been performed, and what advantages this brings for analysis. Fluorescence lifetime imaging (FLIM) is a further extension of time-resolved LIF [30] which has had particularly successful applications in the analysis of works of art and for the assessment of variation in fluorescence lifetime, which can be related to heterogeneities rather than the specific identification of materials which requires careful interpretation of fluorescence and data from complementary analysis. It is therefore recognized that fluorescence and LIF spectroscopy can allow the identification of materials used in cultural heritage only in rare cases; this is due to intrinsic similarities in emission spectra of many materials. In addition, the complex attenuation of fluorescence emission by absorption from other non-fluorescent materials (pigments) is a well-recognized problem and may significantly distort fluorescence spectra [53].

LIF spectroscopy may also be associated within the larger class of LIDAR (light detection and ranging) analyses [143], and a separate section of this work is therefore devoted to a brief description of LIDAR applications involving LIF spectroscopy of buildings and wall paintings [30], which includes fluorescence LIDAR hyperspectral imaging [29].

3.1.1 Basic LIF spectroscopy set-ups

Different set-ups have been proposed for LIF and invariably share common components; (1) a laser source, (2) suitable optics for the delivery of the laser radiation to the sample, (3) a system of lenses (telescope), fibre optics or a combination of the two for the collection of emitted photons, (4) a detector often coupled with a spectrometer or a series of spectral filters. The greatest variability in published set-ups is the laser source and wavelength. Indeed, the excitation source employed in LIF is most related to the type of material being analyzed, and a range of lasers (predominantly, but not exclusively, UV lasers) has been employed for analysis of artists' materials and works of art.

Laser fluences employed for LIF spectroscopy are not rigorously reported, but are generally $\sim$1 mJ cm^{-2} (for example for a 25-ns KrF excimer laser operating at 248 nm) [6] but may be much less (for example 200 μJ cm^{-2} for a 0.5-ns N_2 laser operating at 337 nm [129]). The choice of fluence, or laser power in continuous illumination, should take into account the chemical and thermal sensitivity of the surface (either pigment or organic material) being analyzed, and this is particularly important for sensitive pigments (for example HgS) [66].

For the acquisition of LIF spectra, a filter is placed in front of the detector to eliminate laser light scattered off of the sample surface. Scattered laser radiation can distort emission spectra due to its high intensity that overwhelms fluorescence bringing the detector to saturation or even because of second-order diffraction on the grating used in the spectrometer. In order to avoid collecting radiation from the laser, fibers can be used for collecting anisotropic fluorescence emissions at angles ranging from 60 to 90° with respect to the excitation. Generally, fluorescence emitted by materials of interest in cultural heritage is broad, and therefore a range of detectors based on CCDs with detection ranges from 200 to 1200 nm and spectral resolutions from 0.1 to 10 nm have been used for LIF. A significant advantage of time-gated detectors used in LIF with pulsed laser excitation is that analysis can be performed even in outdoor light conditions (LIDAR) [83].

For the measurement of time-resolved fluorescence emissions, three different instrumental methods and three different fitting procedures have been proposed. Instrumentation has been tested for the analysis of pigments and works of

Table 2 Laser-induced fluorescence of stone (* indicates maximum)

Stone	Laser wavelength/nm	Emission bands/nm	Attribution	Reference(s)
Calcite	266	696, 618*, 591	Eu^{3+}, $^5D_0$–$^7F_2$	[65]
		413, 437, 500–504	Structural defects	[18]
		690–700	Mn^{2+}	[65]
	355	452*	Tm^{3+}	[65]
Buried marble	363	610	Mn^{2+}	[137, 138]
		390*, 380–530	Humic and fulvic acids	

art based on the use of pulsed laser sources (ranging from 200 ps to 5 ns) coupled with (a) a time-resolved streak camera [15], (b) a time-resolved optical multi-channel analyzer (OMA) and ns-delay generator [122, 166] providing spectrally and temporally resolved analysis or (c) a time-correlated single-photon counting (TCSPC) device coupled with suitable filters for analysis of the temporal dependence of a fluorescence emission at a specific wavelength [146]. Obtaining the emission lifetime value(s) best describing the measured emission is done by approximating (fitting) the fluorescence decay experimentally observed with (a) mono- or bi-exponential functions [30, 130], (b) tri-exponential functions [83] or (c) by use of total entropy modelling [147].

3.1.2 Applications of LIF

Both LIF and lamp-based fluorescence spectroscopy have been applied to the study of a range of different materials and works of art, and in many cases attributions for the origin of fluorescence have been suggested. For the purposes of this work, it is useful to classify the different applications of LIF spectroscopy on the basis of the type of material analyzed rather than the wavelength or specific set-up used. Stones and minerals, pigments and colorants, glasses and glazes, varnishes and binding media have all been analyzed in the laboratory using portable (e.g. 337-nm N_2) and research-level but not-easily-transportable (e.g. 248-nm KrF excimer) lasers. For mechanistic studies, LIF spectroscopy has also been applied as a monitoring tool for the assessment of photo-oxidation during laser ablation of model samples (through the use of dopants or through monitoring gas plumes with LIF) of polymers commonly used in conservation and traditional varnishes [16, 17, 133, 172].

Due to the significant research carried out in laboratory studies, it has been possible to extend LIF spectroscopy to measurements in situ and key examples of analysis using LIF and time-resolved spectroscopy of works of art are given. While fluorescence spectroscopy may be unable to resolve complex mixtures, in situ applications highlight how LIF can be useful in pinpointing the location of heterogeneities and, in specific cases, allows the identification of particular materials. Finally, applications of LIDAR for microbiological deterioration on historical buildings and wall paintings are presented.

3.1.2.1 Stone and minerals The fluorescence of natural minerals is usually due to intrinsic defects in their structure or trapped impurities. For this reason, LIF spectroscopy has been applied in the characterization of short and long emissions from calcite (as well as other minerals) [18, 65], a common stone used in sculpture and for the facing of monuments, and fluorescence emission are summarized in Table 2. The analysis of calcite reveals the presence of trace concentrations of ions from transition metals (Mn^{2+}) which dominate the luminescence spectrum of marble, which may also be found with emissions from rare-earth elements (including Tm^{3+} and Eu^{3+}); time-resolved LIF spectroscopy is necessary to resolve the short-lived phosphorescence (recorded at 100 ns following laser excitation and a gate of 0.5–1 μs) contributions from lanthanides, which are normally hidden by the longer-lived (approx. 50 ms) phosphorescence from Mn^{2+} [117]. Archaeological and excavated marble samples have been investigated using LIF spectroscopy to assess changes in fluorescence as a function of burial and following excavation [137, 138]. Indeed, fluorescence of excavated marble has been associated with both Mn^{2+} and the accumulation of humic and fulvic acids which are present in soil.

3.1.2.2 Pigments and colorants Only a few pigments used by artists fluoresce, and impurities (including those found in calcite) may contribute to the fluorescence observed in historical materials. The long-lived phosphorescence reported in other inorganic pigments (for example 0.1 ms for $PbCO_3Pb(OH)_2$ and $Pb(SbO_3)2/Pb_3(Sb_3O_4)_2$ [15]) has not been ascribed to specific fluorophores and may be due to impurities in the studied samples. Many modern semiconductor-based pigments fluoresce, as do organic materials used as pigments and most binding media; these factors make the assignment of fluorescence to specific compounds particularly problematic.

Fluorescent pigments can be classified as natural organic pigments (for example cochineal lakes and sappanwood)

Table 3 LIF spectroscopy of selected pigments

Pigment	Laser wavelength/nm	Emission maxima/nm	Lifetime/ns	Reference(s)
Hansa yellow	337	550		[24]
Sappanwood	337	600		[122]
Cochineal lake	337	630–640		[122]
Curcumin	248, 337	540–560		[25, 122]
Titanium white (TiO_2)	248, 355	473	0.2	[15, 25]
Zinc white (ZnO)	248, 337, 355	385, 530	0.3, 4.4	[6, 15, 38]
Cadmium yellows	337, 355	485–528	0.05–1	[6, 123]
Cadmium reds	355, 337	585–640	0.04–2	[6, 15, 24]
Chrome yellow ($PbCrO_4$)	248, 337	540–580		[24, 25]
Barium yellow ($BaCrO_4$)	248, 337	383, 520		[24]
Vermillion (HgS)	248	607		[24, 66]

[123], synthetic organic pigments (for example di-azo pigments) or synthetic inorganic pigments (including doped glasses and semi-conductor pigments) [6, 15, 142]. A summary of the fluorescence properties of different pigments which have been analyzed with LIF spectroscopy is given in Table 3.

Organic pigments (both synthetic and natural) often fluorescence due to the presence of delocalized electrons in molecules containing multiple aromatic rings (for example anthraquinones), long chains of conjugated double bonds and aromatic rings (curcumin) or di-azo bonds (for example Hansa yellow) [123], and LIF of various organic pigments and dyes has been reported with excitation at 337 nm [121, 123–126]; generally emission bands from organic molecules are broad, which may compromise the differentiation between similar pigments with fluorescence spectroscopy. Measurements of fluorescence lifetime has been proposed as a viable method for discriminating between laccaic acids and carminic acids [83], two anthraquinone pigments which have similar fluorescence emissions but different bi-exponential fluorescence lifetimes.

Semi-conductor pigments including ZnO [15, 24], TiO_2 [15, 126], HgS [24, 66] and cadmium-based yellows and reds [6, 24] emit intense visible photons due to the small band gap, which is responsible for the relatively narrow and short-lived emissions. For cadmium pigments, fluorescence emissions increase in wavelength with increasing concentration of Se [6]. The disparity in the lifetime of fluorescence reported for different semi-conductor pigments is ascribed to the difference in laser pulse duration of the excitation sources used, which ranges from 5 ns (N_2 laser) [126] (suggesting longer lifetimes) to a 300-ps laser (355 nm, third harmonic Nd:YAG) [15] (yielding markedly shorter fluorescence lifetimes for the same pigments). Lead and barium chromates have both been reported to fluoresce, but the origin of this fluorescence is unknown [24, 126].

3.1.2.3 Synthetic fluorescent silicates The strong near-infrared fluorescence emission (centered at approximately 900–950 nm) from Cu-doped silicates (including Egyptian blue and Han blue, materials also used as pigments) has been studied using LIF spectroscopy and has been ascribed to the symmetry-forbidden B_{2g}–B_{1g} transition of Cu^{2+} in a square-planar ligand field, hence the unusually long lifetime [142]. Remarkable quantum yields account for the strong signals found with Egyptian blues, which have been documented in Roman wall paintings using LED-based imaging in situ [122]. Other glasses have been analyzed with LIF spectroscopy: lusters from Renaissance Italian ceramics emit visible broadband luminescence originating most likely from Cu (maximum emission at around 620 nm) and Ag (maximum emission at around 530 nm) nanoclosters; peak shifts observed for different samples studied were attributed to the different metal nanocrystals present in the lustre [106].

3.1.2.4 Varnishes Analysis of varnishes using LIF spectroscopy has been proposed by many (see Table 4) using near-UV laser excitation (337–364.8 nm), and in one case 457.9 nm. Among commonly found varnishes, only shellac has a distinctly different orange-red fluorescence emission from the other varnishes, which allows the rapid discrimination of shellac-based varnishes. The emission maxima of the other varnishes studied occurs between 410 and 490 nm: subtle differences between varnish-based binding media can be appreciated [15, 130] and may depend on the origin (di- or tri-terpenoid), ageing and preparation of the varnishes. The separation of the fluorescence of mixtures of binding media is not possible as detected fluorescence represents a combination of emissions from different media [130]. An effort has been made only in some cases to interpret the fluorescence emissions of varnishes: residual laccaic acids (also used as pigments) are responsible for the strong red-orange emission in shellacs [122, 130] but the identity of

Table 4 Laser-induced fluorescence of varnishes

Varnish	Laser wavelength/nm	Emission maximum/nm	Lifetime/ns	
Amber	337	475		[124]
Colophony	337	420–530	2–8	[130]
		480		[124]
	355	435	17	[15]
Copal	337	405–430	2–9	[130]
		450		[124]
	355	456	6	[15]
Dammar	337	430		[124]
	355	437	7	[15]
Elemi	337	410–480	2–9	[130]
Mastic	337	430–440	2–8	[130]
		450		[124]
	363.8	450		[105]
Sandarac	337	410–460	2–8	[130]
		480		[124]
Shellac	337	430–580	2–9	[130]
		600–640	2–9	[130]
		580, 630	3–5	[124]
	457.9	606, 632, 680		[105]
Turpentine resin	337	410–480	2–9	[130]
	355	450	16	[15]

the fluorophores in other media is not known. Indeed, multiple fluorophores are present in the different media and this is attested to by the wavelength dependence of the fluorescence lifetime of varnishes which has been calculated using a streak camera [15], and the modelling of time-resolved fluorescence spectra using a bi-exponential decay [130]. As for pigments, the difference in the ns-fluorescence lifetimes reported is likely due to the method used for the calculation of the lifetime and the detection of fluorescent photons.

While fluorescence spectroscopy of complex materials like varnishes may not provide satisfying means for the differentiation between varnishes, another important use of the spectra data obtained in LIF is the monitoring of the condition of varnishes as a function of ageing [105]. Further, modelling has demonstrated that detected fluorescence may be influenced by the absorption and reflectance of radiation from underlying layers [53].

3.1.2.5 Binding media Analysis of binding media used as paint has been performed with LIF spectroscopy on a variety of model samples, films and mock-ups of oil- and protein-based binding media and results of various applications of LIF for binding media analysis are summarized in Table 5.

In contrast to the fluorescence of resins used for varnishes, the fluorescence of proteins is better understood, and the identity of different fluorophores has been suggested [128]; protein-based binding media contain many fluorophores, and hence the emission spectra of proteins are strongly dependent on the excitation wavelength. Spectroscopic discrimination between pure protein-based binding media (egg white and casein, egg yolk and animal glues) requires the use of excitation below 300 nm [129, 132], which is sufficiently energetic to excite emissions from aromatic amino acids. When wavelengths greater than 337 nm are employed, spectra recorded of protein-based media are similar in shape, but may differ slightly in fluorescence lifetime [129]. While egg yolk films emit at 425 nm, addition of a drying oil causes a shift to 450 nm [25, 129]. Films of linseed oil exhibit broad fluorescence emissions which shift from 492 to 683 nm [105] with prolonged natural ageing.

In some cases, the addition of pigment to protein-based and oil-based films does not obscure the fluorescence from the binder [24, 66, 105], but the low concentration of binder and the weak signal of amino acid fluorescence limit the ap-

Table 5 LIF spectroscopy of binding media where tryptophan (Trp) and tyrosine (Tyr) attributions are given only when reported

Binding medium	Laser wavelength/nm	Emission wavelength/nm	Lifetime/ns	Attribution	Ref.
Animal glues	248	305, 385		Tyr, pentosodine	[128]
	337	415	4.7	Di-tyrosine	[129]
		430–440			[123]
	355	440, 415, ~480		Pyridinoline, di-tyrosine, dihydroxyphenylalanine and related products	[128]
Calcium caseinate	337	460	6.0		[30]
Casein	248	340, 420		Trp, di-tyrosine	[128]
	266	310, 330		Tyr, Trp	[132]
	355	435		Oxidation products	[128]
	363.8	456			[105]
Egg white	248	340, 420		Trp, di-tyrosine	[128]
	266	310, 330		Tyr, Trp	[132]
	337	415	5.3	Di-tyrosine	[129]
	363.8	588			[105]
	355	435		Oxidation products	[128]
Egg yolk	248	515–440		Phospholipids	[66]
	266	310, 330		Tyr, Trp	[132]
	337	425	4.0		[129]
Egg yolk–linseed oil–tempera	248	450			[24]
Linseed oil–aged 1 year	363.8	492			[105]
Linseed oil–aged 50 years	363.8	685			[105]
Wax	337	500–550	6.0		[30]

plication of LIF for the detection of protein-based binders in paint.

3.1.2.6 Applications in situ: paintings, manuscripts and stone sculptures Despite the numerous studies employing LIF spectroscopy for the analysis of binding media, varnishes and pigments, there are only a few published applications of LIF for the analysis of works of art in situ and this is due to the challenges associated with transporting lasers for analysis; this has been overcome with the introduction of more compact lasers and detectors which can be easily carried in a suitcase for in situ analysis. Easel and wall paintings have been analyzed using portable LIF instrumentation based on a N_2 laser; for example, such a study has revealed anachronistic pigments (ZnO) ascribed to retouching on a painting by Andrea Mantegna [38]. Applications of portable instrumentation for the analysis of fluorescence lifetime have included analysis of fluorescent pigments from the Book of Kells; following analysis of fluorescence of blue and purple pigments using a portable lamp-based system, fluorescence lifetime analysis using a pulsed diode laser confirmed the presence of indigo ($\tau = 2.5$ ns) and orcein ($\tau = 2.4$ ns) [146].

3.1.2.7 Time-resolved fluorescence imaging Fluorescence lifetime imaging (FLIM) is based on the detection of the fluorescence intensity as a function of time with respect to a ns-laser pulse through the use of a time-gated intensified CCD, followed by the application of a mono-exponential fit for the fluorescence decay recorded in each pixel of the image; the calculated fluorescence lifetime is therefore independent of the intensity of the initial fluorescence signal [30]. While FLIM has been used in the study of various binding media [129] and can be used to distinguish pure media on the basis of differences in the lifetime of the fluorescence emission, its most compelling applications are those which have been

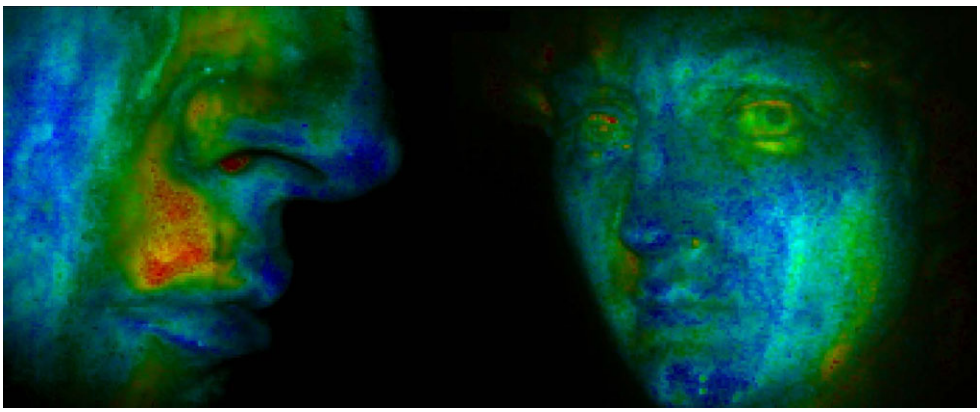

Fig. 2 False color images of results from fluorescence lifetime imaging (FLIM) analysis of Michelangelo's David, demonstrating the presence of residues of organic materials with a fluorescence lifetime which was approximately 6 ns (*red*) compared with the marble substrate with 3 ns (*blue*) © Politecnico di Milano

Table 6 Fluorescence detection using fluorescence–LIDAR

	Laser wavelength/nm	Emission wavelength/nm	Attribution
Buildings and wall paintings	308, 480, 355, 488	570, 660, 680	Phycoerethin, phycocyanin, chlorophyll [10, 83, 110, 174]
	355	440, 520–530	Cells and ferulic acid [83]
		690–740	Plants [83]
	355	680	Chlorophyll [10, 29]

carried out in situ for the imaging of works of art [38]. For example, first applications of FLIM highlighted the presence of drips of beeswax on Michelangelo's David (characterized in parallel using other equipment by a maximum LIF emission at 520 nm) which were mapped with a fluorescence lifetime of approx. 6 ns [30], and details of false color images generated by combining information from calculated fluorescence lifetime and fluorescence intensity are shown in Fig. 2.

Other recent applications of FLIM include the mapping of the distribution of organic materials related to the preparation of gilding in wall paintings [31]; analysis has also revealed the fluorescence from almost invisible decorations on wall paintings by Masolino di Panicale [32].

3.1.2.8 Applications of LIDAR LIF analysis: historical buildings and wall paintings LIDAR analysis using LIF spectroscopy and imaging has included significant studies of external stone and brick buildings from distances between 30 and 300 m [30]; analysis has been performed of areas of the Coliseum [122], the Cathedral in Lund [174] and the Baptistery and Cathedral of Parma [110]. Research has focused on the use of a range of laser wavelengths to detect typical fluorescence from plants (chlorophyll A) and bacteria, and a key aspect of the technique is the detection of points (using a spectrometer) or areas (using a CCD) containing living organisms (summarized in Table 6).

In other applications of LIDAR with LIF, crypt wall paintings have been scanned, and images have been generated using multi-spectral imaging for the mapping of microbiological growth [10, 29]. LIDAR indeed provides major advantages in the assessment of the condition of a monument and wall paintings and, when combined with hyperspectral imaging and statistical analysis, can be particularly useful for the monitoring of microbiological and plant growth with time [30].

3.2 Laser desorption ionization mass spectrometry

Spatially resolved mass spectrometry (MS) analysis of artistic or archaeological objects can be carried out by desorbing charged species from the sample surface with a laser beam. The separation of the desorbed species according to their mass-to-charge ratio is obtained by using a mass analyzer. The lateral resolution of the analysis, typically in the range of dozens of microns (Table 1), is lower than that achieved by using primary ion beams [157]. However, different advantages are associated with the use of laser desorption ionization (LDI) MS, including the softness of the analytical approach and the compatibility with protocols for direct analysis of large objects.

The use of far-UV or IR laser sources with pulse duration in the ns range is important for the direct laser desorption of charged organic species with molecular weights of about 1–2 kDa [140]. For this reason, LDI–MS is often applied as a complementary analytical tool for use in the conservation laboratory alongside techniques such as Fourier transform infrared (FTIR) spectroscopy and micro-Raman spectroscopy [98] for the study of organic components of works of art.

3.2.1 LDI-based techniques

Mass spectrometry methods relying on the LDI process find their origin in 1963 when a pulsed ruby laser (150-µm beam diameter, 50-µs pulse duration) in conjunction with a double-focusing mass spectrometer was used to analyze a variety of solid inorganic compounds [88]. The laser beam interaction with the solid surface caused the vaporization of about 2×10^{17} atoms and created craters 125-µm deep. The subsequent introduction of lasers operating with shorter pulse lengths and reduced spot diameters and fluences increased the mass resolving power of the acquired spectra [85]. Today, the analytical possibilities offered by direct LDI mass spectrometry for the study of non-volatile compounds maintained under vacuum are well known [61] and limitations in investigating large molecules are established.

Limitations suffered by LDI–MS were circumvented in 1987 when matrix-assisted (MA) LDI–MS [95] was introduced by demonstrating that laser desorption ionization can be obtained by mixing the analyte compounds with a surplus of an organic compound (matrix) that is co-desorbed upon laser excitation. The matrix is chosen according to the analyte properties and the laser energy [92] and provides a number of different functions including: (a) isolation of the analyte molecules and preventing their aggregation; (b) absorption of the laser energy via electronic or vibrational excitation (depending on the laser energy); (c) evaporation of un-altered analyte molecules and (d) efficient ionization of analyte molecules [47, 48]. Derivatives of benzoic acid, cinnamic acid and related aromatic compounds are some of the most widely used organic matrices in combination with UV lasers. In particular, the 2,5-dihydroxybenzoic acid and the α-cyano-4-hydroxycinnamic acid act as good UV matrix-assisted laser desorption ionization (MALDI) matrices for a variety of different organic and biomolecular analytes [75]. The interaction of the matrix/analyte mixture with the laser causes a phase transition from solid to gas. The explosive expansion of the gaseous plume mostly disperses neutral species and a reduced amount of ions (few percent) with initial velocity of about 400–800 $m\,s^{-1}$. Very little increase in the internal energy of the analyte occurs as there is little or no fragmentation of the analyte and, thus, MALDI is frequently referred to as a soft ionization technique.

In a typical MALDI analysis, bursts of laser radiation at 10 Hz are focused on the sample through appropriate optics. The N_2 UV laser (337 nm) is the most commonly used one in MALDI; however, infrared lasers offer a good alternative for some applications [26].

MALDI sources are usually coupled with time-of-flight (ToF) mass analyzers because of the inherent pulsed nature of the short temporal (ns) laser sources. The small spatial distribution of desorbed ions further favors the use of ToF analyzers, giving high mass resolution ($M/\Delta M \approx 10{,}000$), high mass accuracy (few ppm) and low detection limits [52]. However, recently, similar performances have also been obtained by using ion trap mass analyzers [162], providing easier access to MS/MS analyses.

LDI and MALDI analyses are typically conducted at the low pressures found in most ion sources (10^{-7}–10^{-8} torr). This environment is useful for ion transfer to the mass analyzer and influences the mechanism by which ions are formed. However, MALDI spectra are also obtained at higher pressures, including atmospheric pressure (AP) [103], by using nitrogen lasers operating at a repetition rate of 10–20 Hz and an average power density of hundreds of $mW\,cm^{-2}$. AP/MALDI analysis using IR sources has also been demonstrated [104].

AP/MALDI analyses are carried out in a manner similar to that for conventional MALDI, with a solid matrix co-crystallized with the analyte. AP/MALDI spectra from solid samples can also be obtained simply following the deposition of a matrix layer on the surface of a sample [73]. Recently, external AP/MALDI sources have been implemented with a number of mass analyzers including ToF [103], ion trap [74] and Fourier transform ion cyclotron resonance (FT ICR) [97]. The external configuration is particularly suitable for the analysis of artistic and archaeological material as it facilitates the analysis of 3D objects [70].

Ions generated by AP/MALDI have been shown to be less energetic than those produced by MALDI and are thus subject to significantly less metastable decay due to fast thermalization of the ion internal energy at atmospheric conditions. However, the reduced ion transmission from the atmosphere into the low vacuum of the mass analyzer produces lower ion current values with respect to MALDI. The ion transmission efficiency depends on both the laser spot displacement relative to the mass analyzer inlet capillary central axis and the voltage applied between the target plate and the inlet capillary. A significant increase in the ion transmission was obtained by adopting an approach called pulsed dynamic focusing (PDF) that involves switching the electric field to zero for a time interval during which ions approach the capillary inlet [165].

The proposed model of AP/MALDI includes ejection of a plume of positive and negative ions after a laser pulse. The ion ejection is followed by ion drifting under the influence of the electric field and gas flow near the inlet to the mass analyzer. Positive ions can also recombine with negative ions during the initial stages of plume expansion. An initial concentration of ions produced by the laser interaction with the sample surface of about 3×10^{11} cm^{-3} (corresponding to about 10^7 ions formed per laser shot) has been estimated on the basis of experiments carried out using a 10-Hz N_2 laser with a focused spot diameter of about 400 µm [12]. An ion transmission efficiency, defined as the ratio of the number

Table 7 LDI-based analyses of art and archaeological materials

Type of material	Technique	Sample	Main signals (m/z)	Ref.
Pigments, dyes	LDI	Phthalocyanine blue (PB15)	575 $[MH]^+$	[14]
		Phthalocyanine green (PG7)	1126 $[MH]^+$	
		Azo pigment PY3	395/397 $[MH]^+$	
		Prussian blue	134 $[Fe(CN)_3]^-$	[79]
		Green pigment G13	247 $[PbK]^+$	
		Carmine lake	104 $[Al_2O_3H_2]^+$	
		Carminic acid	491 $[M–H]^-$	
		Vermilion (HgS)	426 $[HgS_7]^-$, 363$[HgS_5]^-$	[80]
		Orpiment (As_2S_3)	256.6 $[As_3S]^+$	
		Crystal violet	372 $[M]^+$	
		Pigment PR254	357 $[MH]^+$	[98]
		PY65/PY74	386 $[MH]^+$	
	MALDI	Carminic acid	491 $[M–H]^-$	[112]
		Picric acid	228.4 $[M–H]^-$	[156][a]
	AP/MALDI	Iron-gall ink (1,2,3,4,6-pentagalloyl-*O*-D-glucopyranose)	939.1 $[M–H]^-$	[40]
		Crystal violet	372.3 $[M]^+$	[70]
		Acid blue 1	544.5 $[M]^+$	
		Basic blue 7	478.3 $[M]^+$	
		Pigment red 2	434.1 $[M]^+$	
		Acid red 74	372.1 $[M]^+$	
Binding media	MALDI	Linseed oil	Peaks in the region 860–980	[170]
		PEGs in acrylic emulsions		[89]
		Egg	Peptide mass fingerprint	[167]
		Egg white and yolk	Peptide mass fingerprint	[101]
		Carmine dye from *Coccus cacti*	Peptide mass fingerprint	[100]
Varnishes	MALDI	Dammar, mastic	465, 481, 497	[44, 178]
Archaeological samples	MALDI	Oetzi's clothing	Peptide mass fingerprint	[87]

[a]Ref. [156]: results from MALDI analysis of another 58 dyes and pigments are also reported

of ions passing inside the mass analyzer inlet capillary, of about 0.9 was obtained with a laser spot displacement relative to the capillary central axis of 0.2 mm by switching off the extraction voltage 10 µs after the laser pulse.

3.2.2 Applications of LDI-based techniques

Spatially resolved MS techniques based on LDI have been employed in the study of art and archaeological materials since the end of 1990s (Tables 1 and 7) [178].

3.2.2.1 Pigments The use of LDI for pigment analysis started in 2002 when phthalocyanine blue (PB15), phthalocyanine green (PG7) and pigment yellow (PY3) pigments were identified by analyzing a modern acrylic paint applied on a cellulose surface [14, 159]. The analysis was carried out by operating under vacuum conditions with a N_2 laser. Possibilities offered by LDI–MS operating under vacuum conditions in identifying inorganic pigments were also demonstrated by analyzing Prussian blue, lead-containing G13 and carmine lake pigments [79]. Direct LDI–MS analysis of pigments used to paint an illuminated page of the Qur'an (17th century C.E.) and a decorated page of a Hebrew manuscript (19th century C.E.) was performed by introducing the samples into the main source chamber of a ToF spectrometer. The vacuum environment allowed the identification of a variety of pigments including vermilion (HgS) and crystal violet [80]. Unfortunately, the adopted analytical approach can-

not be considered when large samples are analyzed. In fact, the LDI–MS identification of pigments used to paint a group of paintings attributed to Jackson Pollock (1912–1956) was instead carried out by analyzing small samples scraped from the painting surface [98].

MALDI has expanded LDI-based MS methods to studies of organic components in works of art. The use of MALDI–MS for the analysis of organic pigments has often produced results similar to those obtained by LDI–MS. For example, the negative ion MALDI spectrum of carminic acid obtained by using the α-cyano-4-hydroxycinnamic acid matrix shows the same signal at m/z 491 [112] detected with LDI–MS [79] and attributed to the [M–H]–pseudo-molecular ion. Selections of dyes from the Schweppe dye collection and pigments from the Tate Gallery collection were also analyzed by using MALDI–MS [156].

3.2.2.2 Drying oils and terpenoid varnishes The matrix assistance has instead offered new opportunities for the analysis of complex organic systems, widely used in traditional and modern art. Drying oils, also known as siccative oils, are among the oldest binders used in paints. They are mixtures of triesters of glycerol (also called triacylglycerols) with a high content of double and triple unsaturated fatty acids. Prior to their use as binding media for painting, drying oils were often subjected to processes including washing or settling and heating with driers, which caused changes in their original composition [158]. MALDI–MS has been applied to study the changes induced in linseed oil by the above-mentioned processes [170]. In particular, it was found that linseed oil processing may lead to the formation of cross-linked and/or oxidized products and produce triacylglycerol oligomers consisting of up to hexamers.

Naturally occurring triterpenoid resins have been widely used as varnishes in traditional painting. The varnish layer serves as a protective coating for the paint surface and contributes to the final appearance of the painting. Varnish layers are subject to degradation processes that cause their yellowing and alter their mechanical and chemical properties. Aged varnishes become brittle and form cracks. MALDI–MS is a powerful tool to investigate the chemical alterations suffered by aged natural resins. In particular, it has been shown that the principal components of photo-aged dammar and mastic resins can be identified by using graphite-assisted (GA) LDI–MS [44, 178].

3.2.2.3 Modern paints Modern paintings are characterized by the use of various materials including acrylic polymers. The basic formulation of acrylic emulsion paint includes a water emulsion of acrylic polymers. The emulsion contains surfactants added in order to keep the acrylic droplets dispersed in the water during polymerization and storage. Poly(ethylene glycol) (PEG) compounds are the most widely used surfactant in acrylic emulsion paint. MALDI–MS analysis of water extracts of microsamples from a palette by David Hockney (dating from 1970) and sample paintings by Patrick Caulfield (1936–2005) and John Hoyland (born in 1934) were performed in order to characterize the different PEGs used in paint formulation [89]. Surfactants were classified according to their nominal residue mass, weight average molar mass, number average molar mass, polydispersity and relative abundance.

3.2.2.4 Proteins—from paint to archaeological samples The advent of MALDI–MS has provided a significant boost to proteomics research. Peptide mass fingerprint represents the most widely adopted protocol for protein identification. The method takes advantage of the proteolytic activity of selected enzymes to produce a mixture of different peptides as a consequence of the enzymatic digestion of the unknown protein. The MALDI–MS identification of the peptide masses and their comparison to a database containing the known protein sequences allow the precise identification of specific proteins. Peptide mass fingerprint has been used to identify proteinaceous binders used to paint Renaissance paintings [167] and Edward Munch's painting 'Sitting nude and grotesque masque' (dated to 1893) [101]. Small fragments were excised from the paintings' surfaces and analyzed with MALDI–MS after tryptic digestion. Egg was identified as the binder used to paint the selected paintings. The proteomic approach was also tested for the identification of the specific protein present in the *Coccus cacti* insect-derived carmine red dye [100].

The peptide mass fingerprint data were also used to identify biological samples more than 5300 years old, taken from the accoutrement of the Tyrolean mummy (also called Iceman or Oetzi) [87]. In particular, samples from the man's coat and leggings were assigned to sheep while the upper leather of his moccasins was made from cattle. A major drawback for the above-discussed LDI-based analyses of ancient objects is the requirement for medium–high vacuum environment. The vacuum conditions significantly limit the potential for in situ analysis of works of art and archaeological objects.

3.2.2.5 Movable works of art Recently, possibilities offered by AP/MALDI for analyzing portable objects directly in air have been demonstrated by studying traditional materials, iron-gall ink [40] and organic dyes and pigments used to print books dated between 1911 and 1920 [70]. The latter study definitely demonstrated the applicability of AP/MALDI to the study of historical objects as analyses were carried out in situ with a spatial resolution of about 400 µm (Fig. 3). This was achieved by placing books in a modified AP/MALDI source on an XYZ translation table. The microdestructivity of the analysis was

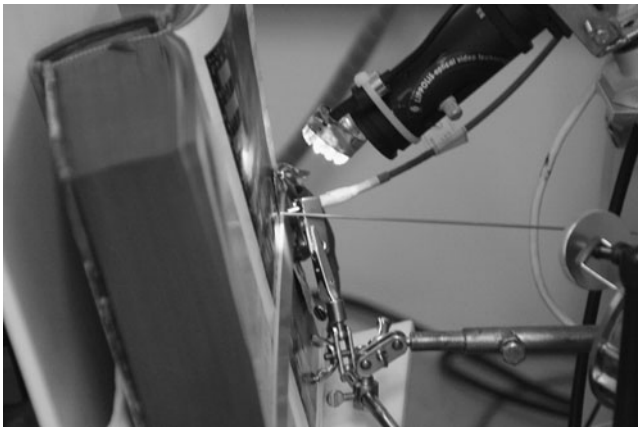

Fig. 3 AP/MALDI MS apparatus used for the direct spatially resolved study of printed books

achieved by spraying about 0.2 $\mu g\,mm^{-2}$ of the 2-[(2E)-3-(4-tert-butylphenyl)-2-methylprop-2-enylidene] malononitrile (DCTB) matrix (corresponding to about 0.8 $nmole\,mm^{-2}$) on a 2–3 mm^2 area of the sample.

4 Combined techniques

In the analysis of works of art, there is often a need to obtain compositional information during object analysis which is as complete as possible; this has led to the use of more than one technique that can supply complementary information. Many examples of multi-technique analysis of cultural heritage materials have been published, but in the majority of cases different analytical instruments and/or experimental set-ups have been employed. Interest among research groups has focused on the exploitation of different techniques in the context of hybrid instruments, which may share common parts and, with minimal adjustments, enable the application of complementary analysis. It is therefore possible to consider the combinations of various spectroscopic techniques, already discussed in this paper, in hybrid instruments. It is emphasized however that while several such combinations have been demonstrated in proof of principle, the commercialization of the multitechniques hybrid instruments would certainly necessitate further development.

4.1 LIF–Raman

An example of such an instrument, actually known for a long time, but not perceived as a hybrid one, is the Raman spectrometer. Using fluorescence emission, which are often observed and actually considered problematic during Raman measurements, may be viewed as a form of hybrid analysis yielding fluorescence spectra along with or instead of Raman spectra on the very same instrument. It has been shown, for example, that Raman scattering and photoluminescence emission, present simultaneously in the same spectrum, could be used for dating artistic glasses from periods corresponding to 1750–1940 A.D. [13]. While no specific Raman resonances or spectral shifts were identified for the dating of the glass, the fluorescence emitted from the glass (excitation: 488 nm) showed a clear increase with age. The origin of this fluorescence was not ascribed but it was noted that the intensity ratio of the Raman band at 1080 cm^{-1} (symmetric stretch of O–Si–O bonds) and the fluorescence signal decreases with time (the logarithm of the ratio was found to have a linear dependence on the age of the glass).

4.2 LIF–LIBS

The similarity of the LIF and LIBS experimental instrumentation is quite obvious and this has allowed the combination, in a single experimental set-up, of these two techniques. As a demonstration, a depth profiling of a model three-layer paint sample was achieved on the basis of both the elemental composition obtained by LIBS and the fluorescence (photoluminescence) of each pigment measured in the successive paint layers [5]. The main requirements for the successful combined implementation of LIF and LIBS is to use a UV laser on the one hand appropriate for exciting organic materials having typically strong absorptions in the UV and on the other hand having adequate pulse energy to produce a proper laser ablation plasma for LIBS analysis.

4.3 LIBS–Raman

This combination may sound awkward on the basis of the differences in LIBS and Raman instrumentation. However, by considering the use of a pulsed instead of cw excitation source for Raman, the instrument similarities become obvious. In fact, instrument development combining LIBS and Raman capabilities has been reported in relation to planetary missions [177]. In the context of cultural heritage studies, a hybrid LIBS–Raman unit has been proposed and tested for pigment analysis, that makes use of a ns pulsed laser at 532 nm for obtaining both Raman and LIBS spectra [68]. The system comprises a relatively simple arrangement of components including the laser source, beam guiding and signal collection optics and a spectrograph–ICCD detection system. By operating the laser at low power levels (pulse energy <0.1 mJ) a Raman spectrum is collected from the sample surface. Increasing the pulse energy above the ablation threshold enables LIBS analysis, which is achieved by a single pulse. This sequence can be repeated if depth profile information is required. A similar system enabling additionally LIBS and Raman, LIF analysis has also been described [132].

A main technical constraint that affects optimization of a LIBS–Raman hybrid concerns the fundamental choice of

laser wavelength. UV or visible excitation (for example, at 355 or 532 nm; Nd:YAG harmonics) could lead to enhanced if not excessive fluorescence that would hamper Raman measurements. Considering NIR excitation at 1064 nm for Raman spectroscopy would result first in significantly reduced scattering cross section compared to visible excitation, but, more importantly, would require a different type of detector sensitive in the 1–2 micron range. To this end, and taking into account the increasing availability of versatile compact spectrometers, it is possible to use two different spectrometers, separately optimized, in a LIBS–Raman hybrid.

4.4 LIBS–XRF

X-ray fluorescence spectroscopy has been among the best choices for obtaining elemental composition information when art and archaeological objects are investigated and recent advances with micro-XRF [91, 93] and portable instrumentation [96] have enhanced such applications considerably.

In a recent study [94], the combined use of micro-XRF and LIBS was investigated. In addition to the use of the techniques independently, special attention was paid to the dynamic combination, involving overlapping the laser beam from a portable LIBS instrument with the X-ray beam from the micro-XRF spectrometer, so as to probe the same point on the object surface. This analysis took place in the context of archaeological metal objects' investigation. LIBS was used first to ablate by successive pulses the corroded metal surface of the artifact and corresponding emission spectra were recorded showing the evolution of LIBS elemental intensities versus depth. In between sets of laser pulses, micro-XRF mapping of the LIBS ablated area was also conducted providing independently the gradient of elemental intensities from the surface towards the bottom of the crater. The elemental mapping of the area ablated by LIBS allowed the evaluation and assessment of the morphological characteristics of the LIBS crater, aiding interpretation of the elemental stratigraphy of the corrosion layer.

4.5 Raman–XRF

XRF analysis has, in several cases, been combined with Raman analysis in an effort by researchers to obtain complete information on material composition [148].

Unlike LIBS or LIF, which are both optical spectroscopies (in the UV and visible or near-IR part of the spectrum), XRF shares no common instrumentation with Raman spectroscopy and as such a hybrid instrument is not feasible. However, both techniques share the general microprobe approach and their combination in a dual unit has been quite an attractive option. Indeed the result of recent development work has led to the construction of a new portable instrument that takes advantage of the simultaneous utilization of both micro-XRF and micro-Raman spectrometry [4]. Initial tests on an overpainted model Byzantine icon have been very encouraging and have demonstrated the instrument's capabilities for in situ and non-invasive identification of pigments. Combining complementary spectral data from the two techniques enables a complete analysis of almost all the pigments present in the painting. Furthermore, in certain cases, in which the overpaint permits adequate penetration of radiation, the XRF analysis is shown to provide valuable information on the underpaint as well. Examination of cross sections is also feasible and then maximum information on the stratigraphy of the paint is obtained.

4.6 LIBS–MS

The species ejected from a solid surface upon laser ablation can be probed by means of either optical emission, namely LIBS, or mass spectrometry, the latter requiring vacuum. However, a dual analytical approach can be followed logically for exploiting both the spectroscopic and the mass analysis of the laser ablation species. Measurements can be carried out within the vacuum chamber of a laser ablation mass spectrometer permitting optical contact with the plume, directly or through an optical fiber. This is straightforward but not necessarily convenient when whole objects are analyzed. Alternatively, it is particularly attractive to consider the combination of LIBS with AP–MALDI, in which case the sample or object is not enclosed within a vacuum chamber.

The combined use of LIBS with laser ablation mass spectrometry has been demonstrated for the analysis of daguerreotypes (photographs on silver-plated copper) that was carried out in two different experimental set-ups [7, 86].

5 Novel laser-based spectroscopic techniques

Various recent advances in laser-based spectroscopy techniques including THz spectroscopy, multi-photon microscopy and time-resolved absorption spectroscopy have triggered new investigations concerning the applications of these new tools in the analysis of artists' materials.

5.1 THz spectroscopy

The terahertz (THz) spectral region lies between approximately 1 and 330 cm^{-1} (0.03–10 THz) and is also known as the far-infrared region. Terahertz radiation is non-ionizing. Recent advances in THz technology concerning both source intensity and detection sensitivity have led to significant signal enhancements. As a result, a number of investigations have focused on new applications of THz spectroscopy in

biophysics and chemistry, and for the analysis of artists' materials [64]. Powerful sources of THz radiation are also available through fs lasers in a broad spectral range, 1–15 THz, and applications have included THz time-domain spectroscopy (TDS) in transmission to probe delocalized (low-frequency) vibrational modes of model samples including binding media and pigments [113]. In another application, reflectance THz spectroscopy has been applied to the analysis of papyrus texts in a limited range of 0.1–1.5 THz [102]. A FT–THz system has been used for the analysis of model artwork in the THz region [62] and a database of FT–THz spectra for pigments and binding media has been published recently [63]. The intense spectral features observed in spectra of artists' materials indicate that THz spectroscopy can be a powerful technique for both qualitative and quantitative analysis of works of art, although interpretation of results can be challenging. The high dynamic range measurements are fundamental as they can allow the analysis of highly absorbing media, and simultaneously enable observations beyond thick varnish layers [63, 64] yielding tomographic images for different materials using the phase information naturally included in the THz electric field measurements.

5.2 Non-linear techniques: multi-photon microscopy

One of the most compelling applications of ultra-fast lasers is the generation of non-linear effects for the analysis of materials made possible by the high power of focused beams. Promising analytical techniques for the analysis of multi-layered works of art include: two- or three-photon excited fluorescence (TPEF), coherent anti-Stokes Raman spectroscopy (CARS) and the non-linear, coherent schemes, such as second- and third-harmonic generation (SHG and THG, respectively). While fs lasers deliver pulses of very high intensities, these pulses are of sufficiently low energies (1 nJ) so that damage and side effects may be minimal. Non-linear techniques are exploited by using microscope objectives for focusing that yields superb localization of excitation ($\sim$0.5 µm) because of the non-linear absorption process involved. Results of analysis using fs pulses at 1028 nm for the generation of TPEF and THG of multi-layered polymer-based materials used in works of art have been reported [56], as has the analysis of canvas linings [57]. An important advantage of these techniques derives from the fact that no energy is absorbed; thus, sample disturbance (e.g. thermal and mechanical side effects) is minimal. SHG can provide information about non-centrosymmetric molecules; THG is generated directly if the axial symmetry along the laser propagation direction is interrupted by a change in material properties, such as by interfaces between materials or layers with different refractive indices.

In multi-photon excited fluorescence analysis, fluorophores with absorption maxima in the visible or in the UV are excited by means of simultaneous absorption of two or three photons in the near IR, and this has been assessed and mapped in multi-layer samples and in oil-varnish systems [131]. Since absorption by most materials employed in artworks in this spectral region is low, the use of NIR light enables deeper optical penetration of the beam and thus makes examination of underlayers feasible. The resolution of multi-photon microscopy is comparable to that provided by confocal microscopy but without the need of using a confocal aperture. By rastering the focused beam in the z-axis (perpendicularly to the artwork surface), highly resolved cross sections and 3D imaging can be obtained.

In another application, a titanium sapphire laser emitting 200-fs pulses at 830 nm which was coupled to a microscope has been used to collect two-photon-excited fluorescence images in the laboratory that allowed the non-invasive detection of paint on an amphora (at the Roman village of Iesso (Guissona), in Catalonia) [34]; analysis provided sufficient signal from barely legible writing, to allow the dating of the amphora.

5.3 Time-resolved absorption spectroscopy

Time-resolved absorption spectroscopy (TRS) has recently been suggested for the analysis of the condition and water content of wood, and current projects focus on extensions of the technique. The measurement of the absorption of photons is particularly complex in diffuse media due to the strong scattering of radiation [164]. TRS has been proposed for the analyses of the absorption and scattering in wood, which are related to the species, moisture content and deterioration of wood [3, 41]. Through the use of a mode-locked ps Ti:sapphire laser emitting pulses between 700 and 1040 nm, diffused photons have been analyzed using a photomultiplier coupled to a TCSPC unit and the system has been applied for the analysis of waterlogged wood [41]. Applications of TRS have also highlighted the change in absorption of wood following dynamic changes in moisture content [42].

6 Conclusions

Laser-based spectroscopic techniques have been applied to the analysis of a range of materials, objects and works of art. Through the careful choice of technique, suitable analytical strategy and set of carefully defined questions, conservators and scientists have been able to better understand specific phenomena on methods for microscopic, molecular and atomic analysis. However, laser-based techniques, like all analytical methods, have specific advantages and intrinsic limitations which have been described in this work, and it is important to carefully choose analytical methods for the

analysis of cultural heritage, which becomes critical in microdestructive and destructive analysis due to limited sample availability. Laser-based methods need to be considered within the wider range of techniques which are available for conservation and archaeological research. One of the major advantages of laser-based techniques is their portability, and examples of applications have been highlighted in this work. With the wider availability of small and (trans)portable powerful laser-based sources spectrometers and detectors for analysis, it is likely that new and exciting applications for the study of cultural heritage materials will be demonstrated and become increasingly accessible to users in the future.

Acknowledgements The authors gratefully acknowledge interactions with co-workers at the Politecnico di Milano, the Università di Catania and IESL-FORTH and the University of Crete, as well as funding from national sources and the European Commission.

References

1. S. Acquaviva, M.L. De Giorgi, C. Marini, R. Poso, J. Cult. Heritage **5**, 365–369 (2004)
2. J. Agresti, A.A. Mencaglia, S. Siano, Anal. Bioanal. Chem. **395**, 2255–2262 (2009)
3. M. Andersson, L. Persson, M. Sjöholm, S. Svanberg, Opt. Express **14**(8), 3641–3653 (2006)
4. K.S. Andrikopoulos, S. Daniilia, B. Roussel, K. Janssens, J. Raman Spectrosc. **37**, 1026–1034 (2006)
5. D. Anglos, Appl. Spectrosc. **55**, 186A–205A (2001)
6. D. Anglos, M. Solomidou, I. Zergioti, V. Zafiropulos, T.G. Papazoglou, C. Fotakis, Appl. Spectrosc. **50**, 1331–1334 (1996)
7. D. Anglos, K. Melessanaki, V. Zafiropulos, M.J. Gresalfi, Appl. Spectrosc. **56**, 423–432 (2002)
8. D. Anglos, S. Georgiou, C. Fotakis, J. Nanopart. Res. **8**, 47–60 (2009)
9. J.M. Anzano, M.A. Villoria, I.B. Gornushkin, B.W. Smith, J.D. Winefordner, Can. J. Anal. Sci. Spectrosc. **47**, 134–140 (2002)
10. P. Aristipini, F. Colao, R. Fantoni, L. Fiorani, A. Palucci, Proc. SPIE **203**, 196–203 (2005)
11. J. Baker, S. Stos, T. Waight, Archaeometry **48**, 45–56 (2006)
12. V.D. Berkout, S.I. Kryuchkov, V.M. Doroshenko, Rapid Commun. Mass Spectrom. **21**, 2046–2050 (2007)
13. A. Bertoluzza, S. Cacciari, G. Cristini, C. Fagnano, A. Tinti, J. Raman Spectrosc. **26**, 751–755 (1995)
14. J.J. Boon, T. Learner, J. Anal. Appl. Pyrolysis **64**, 327–344 (2002)
15. I. Borgia, R. Fantoni, C. Flamini, T.M.D. Palma, A.G. Guidoni, A. Mele, Appl. Surf. Sci. **127–129**, 95–100 (1998)
16. G. Bounos, A. Kolloch, T. Stergiannakos, E. Varatsikou, S. Georgiou, J. Appl. Phys. **98**, 1–9 (2005)
17. G. Bounos, A. Selimis, S. Georgiou, E. Rebollar, M. Castillejo, N. Bityurin, J. Appl. Phys. **100**, 114323 (2006)
18. B.J. Bozlee, A.K. Misra, S.K. Sharma, M. Ingram, Spectrochim. Acta, Part A, Mol. Biomol. Spectrosc. **61**, 2342–2348 (2005)
19. R.G. Brewer, A. Mooradian, B.P. Stoicheff, Phys. Today **60**, 49–55 (2007)
20. L.B. Brostoff, J.J. Gonzalez, P. Jett, R.E. Russo, J. Archaeol. Sci. **36**, 461–466 (2009)
21. A. Brysbaert, K. Melessanaki, D. Anglos, J. Archaeol. Sci. **33**, 1095–1104 (2006)
22. L. Burgio, K. Melessanaki, M. Doulgeridis, R.J.H. Clark, D. Anglos, Spectrochim. Acta B **56**, 905–913 (2001)
23. N. Carmona, M. Oujja, E. Rebollar, H. Romich, M. Castillejo, Spectrochim. Acta B **60**, 1155–1162 (2005)
24. M. Castillejo, M. Martín, M. Oujja, D. Silva, R. Torres, C. Domingo, J.V. García-Ramos, S. Sánchez-Cortés, Appl. Spectrosc. **55**, 992–998 (2001)
25. M. Castillejo, M. Martin, M. Oujia, D. Silva, R. Torres, A. Manousaki, V. Zafiropulos, O.F. Van den Brink, R.M. Heeren, R. Teule, A. Silva, H. Gouveia, Anal. Chem. **74**, 4662–4671 (2002)
26. M. Christoph, K. Dreisewerd, S. Berkenkamp, F. Hillenkamp, J. Am. Soc. Mass Spectrom. **13**, 975 (2002)
27. E. Ciliberto, G. Spoto, Modern analytical methods in art and archaeology, in *Chemical Analysis*. A Series of Monographs on Analytical Chemistry and its Applications, vol. 155, ed. by J.D. Winefordner (Wiley, New York, 2000)
28. A. Ciucci, M. Corsi, V. Palleschi, S. Rastelli, A. Salvetti, E. Tognoni, Appl. Spectrosc. **53**, 960–964 (1999)
29. F. Colao, R. Fantoni, L. Fiorani, A. Palucci, I. Gomoiu, R. Academy, S. Independentei, J. Optoelectron. Adv. Mater. **7**, 3197–3208 (2005)
30. D. Comelli, C.D. Andrea, G. Valentini, R. Cubeddu, C. Colombo, L. Toniolo, Appl. Opt. **43**, 2175–2183 (2004)
31. D. Comelli, G. Valentini, R. Cubeddu, L. Toniolo, Appl. Spectrosc. **59**, 1174–1181 (2005)
32. D. Comelli, A. Nevin, G. Valentini, I. Osticioli, E.M. Castellucci, L. Toniolo, D. Gulotta, R. Cubeddu, J. Cult. Heritage **12**(1), 11–18 (2010)
33. M. Cooper, *Laser Cleaning* (Butterworth-Heinemann, Oxford, 1998)
34. I.G. Cormack, P. Loza-Alvarez, L. Sarrado, S. Tomás, I. Amat-Roldan, L. Torner, D. Artigas, J. Guitart, J. Pera, J. Ros, J. Archaeol. Sci. **34**, 1594–1600 (2007)
35. M. Corsi, G. Cristoforetti, V. Palleschi, A. Salvetti, E. Tognoni, Eur. Phys. J. D **13**, 373–377 (2001)
36. M. Corsi, G. Cristoforetti, M. Giuffrida, M. Hidalgo, S. Legnaioli, L. Masotti, V. Palleschi, A. Salvetti, E. Tognoni, C. Vallebona, A. Zanini, Microchim. Acta **152**, 105–111 (2005)
37. D.A. Cremers, L.J. Radziemski, *Handbook of Laser-Induced Breakdown Spectroscopy* (Wiley, New York, 2006)
38. R. Cubeddu, D. Comelli, G. Valentini, L. Toniolo, La spettroscopia di fluorescenza UV: ritocchi e trattamenti, in *Andrea Mantegna, La pala di San Zeno, la pala Trivulzio. Conoscenza, Conservazione, Monitoraggio*, ed. by F. Pesci, L. Toniolo (Marsilio Editore, Venezia, 2008)
39. J. Cunat, S. Palanco, F. Carrasco, M.D. Simon, J.J. Laserna, J. Anal. At. Spectrom. **20**, 295–300 (2005)
40. R. D'Agata, G. Grasso, S. Parlato, S. Simone, G. Spoto, Appl. Phys. A **89**, 91–95 (2007)
41. C. D'Andrea, A. Farina, D. Comelli, A. Pifferi, P. Taroni, G. Valentini, R. Cubeddu, L. Zoia, M. Orlandi, A. Kienle, Appl. Spectrosc. **62**(5), 569–574 (2008)
42. C. D'Andrea, A. Nevin, A. Farina, A. Bassi, R. Cubeddu, Appl. Opt. **48**(4), B87–B93 (2009)
43. A. De Giacomo, M. Dell'Aglio, A. Casavola, G. Colonna, O. De Pascale, M. Capitelli, Anal. Bioanal. Chem. **385**, 303–311 (2006)
44. P. Dietemann, M. Kälin, S. Zumbühl, R. Knochenmuss, S. Wülfert, R. Zenobi, Anal. Chem. **73**, 2087–2096 (2001)
45. B. Dolgin, Y. Chen, V. Bulatov, I. Schechter, Anal. Bioanal. Chem. **386**, 1535–1541 (2006)
46. J.-C. Dran, J. Salomon, T. Calligaro, P. Walter, Nucl. Instrum. Methods Phys. Res. B **219–220**, 7–15 (2004)
47. K. Dreisewerd, Chem. Rev. **103**, 395–425 (2003)
48. K. Dreisewerd, S. Berkenkamp, A. Leisner, A. Rohlfing, C. Menzel, Int. J. Mass Spectrom. **226**, 189–209 (2003)
49. S.F. Durrant, J. Anal. At. Spectrom. **14**, 1385–1403 (1999)

50. L. Dussubieux, A. Deraisme, G. Frot, C. Stevenson, A. Creech, Y. Bienvenu, Archaeometry **50**, 643–657 (2008)
51. L. Dussubieux, C.M. Kusimba, V. Gogte, S.B. Kusimba, B. Gratuze, R. Oka, Archaeometry **50**, 797–821 (2008)
52. R.D. Edmondson, D. Russell, J. Am. Soc. Mass Spectrom. **7**, 995–1001 (1996)
53. M. Elias, C. Magnain, C. Barthou, D. Comelli, A. Nevin, G. Valentini, Proc. SPIE **7391**, 739104 (2009)
54. A. Erdem, A. Çilingiroğlu, A. Giakoumaki, M. Castanys, E. Kartsonaki, C. Fotakis, D. Anglos, J. Archaeol. Sci. **35**, 2486–2494 (2008)
55. B. Fernández, F. Claverie, C. Pécheyran, O.F.X. Donard, F. Claverie, TrAC, Trends Anal. Chem. **26**, 951–966 (2007)
56. G. Filippidis, E.J. Gualda, K. Melessanaki, C. Fotakis, Opt. Lett. **33**, 240–242 (2008)
57. G. Filippidis, K. Melessanaki, C. Fotakis, Anal. Bioanal. Chem. **395**, 2161–2166 (2009)
58. F.J. Fortes, M. Cortes, M.D. Simon, L.M. Cabalin, J.J. Laserna, Anal. Chim. Acta **554**, 136 (2005)
59. F.J. Fortes, J. Cuñat, L.M. Cabalín, J.J. Laserna, Appl. Spectrosc. **61**, 558 (2007)
60. C. Fotakis, D. Anglos, V. Zafiropulos, S. Georgiou, V. Tornari, *Lasers in the Preservation of Cultural Heritage. Principles and Applications* (Taylor and Francis, New York, 2006)
61. A. Frédéric, Anal. Bioanal. Chem. **389**, 1381–1396 (2007)
62. K. Fukunaga, E-Conserv. Mag. **10**, 30–42 (2009)
63. K. Fukunaga, M. Piccolo, Appl. Phys. A **100**, 591–597 (2010)
64. K. Fukunaga, Y. Ogawa, S. Hayashi, I. Hosako, IEICE Electron. Express **4**, 258–263 (2007)
65. M. Gaft, G. Panczer, R. Reisfeld, Phys. Chem. Miner. **28**, 347–363 (2001)
66. S. Gaspard, M. Oujja, P. Moreno, C. Mendez, A. Garcia, C. Domingo, M. Castillejo, Appl. Surf. Sci. **255**, 2675–2681 (2008)
67. S. Georgiou, A. Koubenakis, Chem. Rev. **103**, 349–393 (2003)
68. A. Giakoumaki, I. Osticioli, D. Anglos, Appl. Phys. A **83**, 537–541 (2006)
69. A. Giakoumaki, K. Melessanaki, D. Anglos, Anal. Bioanal. Chem. **387**, 749–760 (2007)
70. L. Giurato, A. Candura, G. Grasso, G. Spoto, Appl. Phys. A **97**, 263–269 (2009)
71. B. Giussani, D. Monticelli, L. Rampazzi, Anal. Chim. Acta **635**, 6–21 (2009)
72. I. Gobernado-Mitre, A.C. Prieto, V. Zafiropulos, Y. Spetsidou, C. Fotakis, Appl. Spectrosc. **51**(8), 1125–1129 (1997)
73. G. Grasso, M. Fragai, E. Rizzarelli, G. Spoto, K.J. Yeo, J. Mass Spectrom. **41**, 1561–1569 (2006)
74. G. Grasso, E. Rizzarelli, G. Spoto, J. Mass Spectrom. **42**, 1590–1598 (2007)
75. G. Grasso, P. Mineo, E. Rizzarelli, G. Spoto, Int. J. Mass Spectrom. **282**, 50–55 (2009)
76. B. Gratuze, M. Blet-Lemarquand, J.N. Barrandon, J. Radioanal. Nucl. Chem. **247**, 645–656 (2001)
77. A.L. Gray, Analyst **110**, 551–556 (1985)
78. R.L. Green, R.J. Watling, J. Forensic Sci. **52**, 851–859 (2007)
79. D.M. Grim, J. Allison, Int. J. Mass Spectrom. **222**, 85–99 (2003)
80. D.M. Grim, J. Allison, Archaeometry **46**, 283–299 (2004)
81. R. Gronlund, M. Lundqvist, S. Svanberg, Opt. Lett. **30**, 2882 (2005)
82. M.F. Guerra, T. Calligaro, J. Archaeol. Sci. **31**, 1199–1208 (2004)
83. J. Hällström, K. Barup, R. Grönlund, A. Johansson, S. Svanberg, L. Palombi, D. Lognoli, V. Raimondi, G. Cecchi, C. Conti, J. Cult. Heritage **10**, 106–115 (2009)
84. R.S. Harmon, F.C. DeLucia, C.E. McManus, N.J. McMillan, T.F. Jenkins, M.E. Walsh, A. Miziolek, Appl. Geochem. **21**, 730–747 (2006)
85. F. Hillenkamp, E. Unsöld, F. Kaufmann, R. Nitsche, Nature **256**, 119–120 (1975)
86. D.L. Hogan, V.V. Golovlev, M.J. Gresalfi, J.A. Chaney, C.S. Feigerle, J.C. Miller, G. Romer, P. Messier, Appl. Spectrosc. **53**, 1161–1168 (1999)
87. K. Hollemeyer, W. Altmeyer, E. Heinzle, C. Pitra, Rapid Commun. Mass Spectrom. **22**, 2751–2767 (2008)
88. R.E. Honig, J.R. Woolston, Appl. Phys. Lett. **2**, 138–139 (1963)
89. F.G. Hoogland, J.J. Boon, Int. J. Mass Spectrom. **284**, 72–80 (2009)
90. Z.C. Hu, Y.S. Liu, L. Chen, L.A. Zhou, M. Li, K.Q. Zong, L.Y. Zhu, S. Gao, J. Anal. At. Spectrom. **26**, 425–430 (2011)
91. K. Janssens, G. Vittiglio, I. Deraedt, A. Aerts, B. Vekenmans, L. Vincze, F. Wei, I. Deryck, O. Schalm, F. Adams, A. Rindby, A. Knöchel, A. Simionovici, A. Snigirev, X-Ray Spectrom. **29**, 73–91 (2000)
92. J. Kampmeier, K. Dreisewerd, M. Schurenberg, K. Strupat, Int. J. Mass Spectrom. **169–170**, 31–41 (1997)
93. B. Kanngiesser, W. Malzer, A. Fuentes Rodriguez, I. Reiche, Spectrochim. Acta, Part B, At. Spectrosc., **60**, 41–47 (2005)
94. V. Kantarelou, C. Zarkadas, A. Giakoumaki, M. Giannoulaki, A.G. Karydas, D. Anglos, V. Argyropoulos, A novel approach on the combined *in-situ* application of LIBS and μ-XRF spectrometers for the characterization of copper alloy corrosion products, in *Proc. Metal 2007, METAL-07*, Amsterdam, The Netherlands, 17–21 September 2007. Innovative Investigation of Metal Artifacts, vol. 2 (2007), pp. 35–41
95. M. Karas, D. Bachmann, U. Bahr, F. Hillenkamp, Int. J. Mass Spectrom. Ion Process. **78**, 53–68 (1987)
96. A.G. Karydas, D. Kotzamani, R. Bernard, J.N. Barrandon, Ch. Zarkadas, Nucl. Instrum. Methods Phys. Res., Sect. B, Beam Interact. Mater. Atoms **226**, 15–28 (2004)
97. K.A. Kellersberger, P.V. Tan, V.V. Laiko, V.M. Doroshenko, D. Fabris, Anal. Chem. **76**, 3930–3934 (2004)
98. D.P. Kirby, N. Khandekar, K. Sutherland, B.A. Price, Int. J. Mass Spectrom. **284**, 115–122 (2009)
99. S. Klein, T. Stratoudaki, V. Zafiropulos, J. Hildenhagen, K. Dickmann, Th. Lehmkuhl, Appl. Phys. A **69**, 441–444 (1999)
100. S. Kuckova, I. Nemec, R. Hynek, J. Hradilova, T. Grygar, Anal. Bioanal. Chem. **382**, 275–282 (2005)
101. S. Kuckova, R. Hynek, M. Kodicek, Anal. Bioanal. Chem. **388**, 201–206 (2007)
102. J. Labaune, J.B. Jackson, S. Pagès-Camagna, I.N. Duling, M. Menu, G.A. Mourou, Appl. Phys. A **100**, 607–612 (2010)
103. V.V. Laiko, M.A. Baldwin, A.L. Burlingame, Anal. Chem. **72**, 652–657 (2000)
104. V.V. Laiko, N.I. Taranenko, V.D. Berkout, M.A. Yakshin, C.R. Prasad, H.S. Lee, V.M. Doroshenko, J. Am. Soc. Mass Spectrom. **13**, 354–361 (2002)
105. L.J. Larson, K.-S.K. Shin, J.I. Zink, J. Am. Inst. Conserv. **30**, 89–104 (1991)
106. V. Lazic, F. Colao, R. Fantoni, A. Palucci, V. Spizzichino, I. Borgia, B.G. Brunetti, A. Sgamellotti, J. Cult. Heritage **4**, 303–308 (2003)
107. V. Lazic, R. Fantoni, F. Colao, A. Santagata, A. Morona, V. Spizzichino, J. Anal. At. Spectrom. **19**, 429–436 (2004)
108. V. Lazic, F. Colao, R. Fantoni, V. Spizzichino, Spectrochim. Acta B **60**, 1014–1024 (2005)
109. T.J. Lie, K.H. Kurniawan, D.P. Kurniawan, M. Pardede, M.M. Suliyanti, A. Khumaeni, S.A. Natiq, S.N. Abdulmadjid, Y.I. Lee, K. Kagawa, N. Idris, M.O. Tjia, Spectrochim. Acta, Part B, At. Spectrosc. **61**, 104–112 (2006)
110. D. Lognoli, G. Cecchi, I. Mochi, L. Pantani, V. Raimondi, R. Chiari, T. Johansson, P. Weibring, H. Edner, S. Svanberg, Appl. Phys. B **465**, 457–465 (2003)
111. A.J. Lopez, G. Nicolas, M.P. Mateo, V. Pinon, M.J. Vobar, A. Ramil, Spectrochim. Acta B **60**, 1149–1154 (2005)

112. M.S. Maier, S.D. Parera, A.M. Seldes, Int. J. Mass Spectrom. **232**, 225–229 (2004)
113. J.-M. Manceau, A. Nevin, C. Fotakis, S. Tzortzakis, Appl. Phys. B **90**, 365–368 (2008)
114. M. Mantler, M. Schreiner, X-Ray Spectrom. **29**, 3–17 (2000)
115. P.V. Maravelaki, V. Zafiropulos, V. Kylikoglou, M. Kalaitzaki, C. Fotakis, Spectrochim. Acta B **52**, 41–53 (1997)
116. P.V. Maravelaki-Kalaitzaki, D. Anglos, V. Kylikoglou, V. Zafiropulos, Spectrochim. Acta B **56**, 887–903 (2001)
117. R. Mason, M. Clouter, R. Goulding, Phys. Chem. Miner., **32**, 451–459 (2005)
118. K. Melessanaki, M. Panagiotaki, S. Chlouveraki, P.P. Betancourt, D. Anglos, Analysis of Bronze Age vitreous materials. Experience with a new LIBS instrument, Poster presentation, in *International Conference "Laser Induced Breakdown Spectroscopy"*, Orlando, FL, USA (2002)
119. D. Menut, P. Fichet, J. Lacour, A. Rivoallan, P. Mauchien, Appl. Opt. **42**, 6063–6071 (2003)
120. P. Mirti, Ann. Chim. **79**, 455–477 (1989)
121. T. Miyoshi, Jpn. J. Appl. Phys. **24**, 1113–1114 (1985)
122. T. Miyoshi, Jpn. J. Appl. Phys. **26**, 780–781 (1987)
123. T. Miyoshi, Jpn. J. Appl. Phys. **27**, 627–630 (1988)
124. T. Miyoshi, Jpn. J. Appl. Phys. **29**, 1727–1728 (1990)
125. T. Miyoshi, Y. Matsuda, Jpn. J. Appl. Phys. **26**, 239–245 (1987)
126. T. Miyoshi, M. Ikeya, S. Kinoshita, T. Kushida, Jpn. J. Appl. Phys. **21**, 1032–1036 (1982)
127. K. Müller, H. Stege, Archaeometry **45**, 421–433 (2003)
128. A. Nevin, S. Cather, D. Anglos, C. Fotakis, Anal. Chim. Acta **573–574**, 341–346 (2006)
129. A. Nevin, D. Comelli, G. Valentini, D. Anglos, A. Burnstock, S. Cather, R. Cubeddu, Anal. Bioanal. Chem. **388**, 1897–1905 (2007)
130. A. Nevin, J.-P. Echard, M. Thoury, D. Comelli, G. Valentini, R. Cubeddu, Talanta **80**, 286–293 (2009)
131. A. Nevin, D. Comelli, I. Osticioli, G. Filippidis, K. Melessanaki, G. Valentini, R. Cubeddu, C. Fotakis, Appl. Phys. A **100**, 599–606 (2010)
132. I. Osticioli, N.F.C. Mendes, A. Nevin, A. Zoppi, C. Lofrumento, M. Becucci, E.M. Castellucci, Rev. Sci. Instrum. **80**, 076109 (2009)
133. M. Oujja, E. Rebollar, M. Castillejo, Appl. Surf. Sci. **211**, 128–135 (2003)
134. S. Palanco, J.J. Laserna, Rev. Sci. Instrum. **75**, 2068–2074 (2004)
135. D.G. Papazoglou, V. Papadakis, D. Anglos, J. Anal. At. Spectrom. **19**, 483–488 (2004)
136. J. Pérez-Arantegui, M. Resano, E. Garcìa-Ruiz, F. Vanhaecke, C. Roldán, J. Ferrero, J. Coll, Talanta **74**, 1271–1280 (2008)
137. K. Polikreti, C. Christofides, Appl. Phys. A **90**, 285–291 (2007)
138. K. Polikreti, C. Christofides, Archaeometry **52**, 937–948 (2010)
139. A.M. Pollard, C. Heron, *Archaeological Chemistry* (Royal Society of Chemistry, Cambridge, 1996)
140. M.A. Posthumus, P.G. Kistemaker, H.L.C. Meuzelaar, Anal. Chem. **50**, 985–991 (1978)
141. P. Pouli, A. Selimis, S. Georgiou, C. Fotakis, Acc. Chem. Res. **43**, 771–781 (2010)
142. G. Pozza, D. Ajò, G. Chiari, F. De Zuane, M. Favaro, J. Cult. Heritage **1**, 393–398 (2000)
143. V. Raimondi, G. Cecchi, D. Lognoli, L. Palombi, R. Grönlund, A. Johansson, S. Svanberg, K. Barup, J. Hällström, Int. Biodeterior. Biodegrad. **63**, 823–835 (2009)
144. M. Resano, E. García-Ruiz, R. Alloza, M.P. Marzo, P. Vandenabeele, F. Vanhaecke, Anal. Chem. **79**, 8947–8955 (2007)
145. M. Resano, E. García-Ruiz, F. Vanhaecke, Mass Spectrom. Rev. **29**, 55–78 (2009)
146. A. Romani, C. Clementi, C. Miliani, B.G. Brunetti, A. Sgamellotti, G. Favaro, Appl. Spectrosc. **62**, 1395–1399 (2008)
147. A. Romani, C. Clementi, C. Miliani, G. Favaro, Acc. Chem. Res. **43**, 837–846 (2010)
148. F. Rosi, C. Miliani, I. Borgia, B. Brunetti, A. Sgamelotti, J. Raman Spectrosc. **35**, 610–615 (2004)
149. R.E. Russo, X.L. Mao, O.V. Borisov, Liu Haichen, J. Anal. At. Spectrom. **15**, 1115–1120 (2000)
150. R. Salimbeni, R. Pini, S. Siano, Spectrochim. Acta B **56**, 877–885 (2001)
151. O. Samek, D.C.S. Beddows, H.H. Telle, J. Kaiser, M. Liska, J.O. Caseres, A. Gonzales Urena, Spectrochim. Acta B **56**, 865–875 (2001)
152. G. Sarah, B. Gratuze, J.N. Barrandon, J. Anal. At. Spectrom. **22**, 1163–1167 (2007)
153. J. Scaffidi, S.M. Angel, D.A. Cremers, Anal. Chem. **78**, 25–32 (2006)
154. A. Shortland, N. Rogers, K. Eremin, J. Archaeol. Sci. **34**, 781–789 (2007)
155. S. Siano, R. Salimbeni, Acc. Chem. Res. **43**, 733–750 (2010)
156. L.J. Soltzberg, A. Hagar, S. Kridaratikorn, A. Mattson, R. Newman, J. Am. Soc. Mass Spectrom. **18**, 2001–2006 (2007)
157. G. Spoto, Thermochim. Acta **365**, 157–166 (2000)
158. G. Spoto, Acc. Chem. Res. **35**, 652–659 (2002)
159. G. Spoto, G. Grasso, TrAC, Trends Anal. Chem. **30**, 856–863 (2011)
160. G. Spoto, A. Torrisi, A. Contino, Chem. Soc. Rev. **29**, 429–439 (2000)
161. C. Stadlbauer, C. Reiter, B. Patzak, G. Stingeder, T. Prohaska, Anal. Bioanal. Chem. **388**, 593–602 (2007)
162. K. Strupat, V. Kovtoun, H. Bui, R. Viner, G. Stafford, S. Horning, J. Am. Soc. Mass Spectrom. **20**, 1451–1463 (2009)
163. M.M. Suliyanti, S. Sardy, A. Kusnowo, M. Pardede, R. Hedwig, K.H. Kurniawan, T.J. Lie, D.P. Kurniawan, K. Kagawa, J. Appl. Phys. **98**, 093307 (2005)
164. S. Svanberg, Appl. Phys. B **92**, 351–358 (2008)
165. P.V. Tan, V.V. Laiko, V.M. Doroshenko, Anal. Chem. **76**, 2462–2469 (2004)
166. M. Thoury, J.-P. Echard, M. Réfrégiers, B. Berrie, A. Nevin, F. Jamme, L. Bertrand, Anal. Chem. **83**, 1737–1745 (2011)
167. C. Tokarski, E. Martin, C. Rolando, C. Cren-Olivé, Anal. Chem. **78**, 1494–1502 (2006)
168. S. Tzortzakis, D. Gray, D. Anglos, Opt. Lett. **31**, 1139 (2006)
169. K. Ulens, L. Moens, R. Dams, S. Van Winckel, L. Vandevelde, J. Anal. At. Spectrom. **9**, 1243–1248 (1994)
170. J.D.J. Van Den Berg, N.D. Vermist, L. Carlyle, M. Holèapek, J.J. Boon, J. Sep. Sci. **28**, 181–199 (2004)
171. P. Vandenabeele, H.G.M. Edwards, L. Moens, Chem. Rev. **107**, 675–686 (2007)
172. P. Vounisiou, A. Selimis, G.J. Tserevelakis, K. Melessanaki, P. Pouli, G. Filippidis, C. Beltsios, S. Georgiou, C. Fotakis, Appl. Phys. A **100**, 647–652 (2010)
173. B. Wagner, E. Bulska, J. Anal. At. Spectrom. **19**, 1325–1329 (2004)
174. P. Weibring, T. Johansson, H. Edner, S. Svanberg, B. Sundnér, V. Raimondi, G. Cecchi, L. Pantani, Appl. Opt. **40**, 6111–6120 (2001)
175. P. Westlake, P. Siozos, A. Philippidis, Ch. Apostolaki, B. Derham, A. Terlixi, V. Perdikatsis, R. Jones, D. Anglos, Anal. Bioanal. Chem. (2011). doi:10.1007/s00216-011-5281-z
176. A.R. Whitaker, J.W. Eerkens, A.M. Spurling, E.L. Smith, M.A. Gras, J. Archaeol. Sci. **35**, 1104–1113 (2008)
177. R.C. Wiens, S.K. Sharma, J. Thompson, A. Misra, P.G. Lucey, Spectrochim. Acta A **61**, 2324–2334 (2005)
178. S. Zumbühl, R. Knochenmuss, S. Wülfert, F. Dubois, M.J. Dale, R. Zenobi, Anal. Chem. **70**, 707–715 (1998)